A Study on the Ion Channel Dynamics Using the Minimal Diffusion Formulation Variants 2v1n and 1v1n

Hemin Sardar Abdulla

Submitted to the
Institute of Graduate Studies and Research
in partial fulfillment of the requirements for the degree of

Master of Science
in
Computer Engineering

Eastern Mediterranean University
January 2018
Gazimağusa, North Cyprus

Approval of the Institute of Graduate Studies and Research

Assoc. Prof. Dr. Ali Hakan Ulusoy
Acting Director

I certify that this thesis satisfies the requirements as a thesis for the degree of Master of Science in Computer Engineering.

Prof. Dr. Işık Aybay
Chair, Department of Computer Engineering

We certify that we have read this thesis and that in our opinion it is fully adequate in scope and quality as a thesis for the degree of Master of Science in Computer Engineering.

Prof. Dr. Marifi Güler
Supervisor

Examining Committee

1. Prof. Dr. Marifi Güler

2. Assoc. Prof. Dr. Muhammed Salamah

3. Asst. Prof. Dr. Mehtap Köse Ulukök

ABSTRACT

The excitability of cells will be facilitated by voltage–gated ion channels. Although, these channels are accommodating individually by a multiple number of gates. The effects of ion channel fluctuations on the transmembrane voltage activity are profound of small-size membranes patches.

Recently, a model that captures the collective dynamics of Markov chain ensembles was proposed by Güler, M. (2015) [*Physical Review E*, 91(6), 062116] under the name "Minimal diffusion formulation of Markov chain ensembles". Additionally, two simpler variants of it. Called 2v1n and 1v1n formulations, were introduced by the same author [*Physical Review E*, 93(2), 022123].

By applying the minimal diffusion formulation to the gating dynamics which is in ion channel clusters and it was seen that the formulation accurately describes the excitability of neurons. On the other hand, the 2v1n and 1v1n formulations' performance for the ion channel clusters are not examined.

In this thesis, a study on the neural dynamics is performed using the 2v1n and 1v1n formulation. The study examined the accuracy of the formulation by numerical simulation. In doing so, the exact microscopic dynamic simulations of the ion channel cluster were taken as the reference point.

Keywords: Ion Channel, Channel Noise, Stochastic Hodgkin-Huxley, Markov chain, Minimal diffusion formulation.

ÖZ

Nöron uyarılmasını hücre zarında bulunan ve voltaj bağımlı geçirgenlik sergileyen iyon kanalları sağlar. İyon kanal dalgalanmaları küçük boyutlu hücre zarlarındaki voltaj farkı üzerinde hayati etki yapabilmektedir.

Son yıllarda, toplu Markov zincir dinamiği üzerine "Minimal Markov zincir difüzyon formülasyonu" adı altında Güler, M. (2015) tarafından bir model ortaya konulmuştur [*Physical Review E*, 91(6), 062116]. Ayrıca, aynı yazar tarafından, bu modelin daha basit iki formulasyonu olan 2v1n and 1v1n adıyla bilinen varyasyonları ortaya konulmuştur [*Physical Review E,* 93(2), 022123].

Minimal difüzyon formülasyonu, iyon kanallarının dinamiğine uygulanmış ve hayli başarılı sonuçlar gözlenmiştir. Ancak, 2v1n and 1v1n formulasyonları, iyon kanallarının dinamiğine uygulanmamıştır.

Bu tezde, iyon kanal dinamiği, 2v1n and 1v1n formulasyonları kullanarak sayısal olarak çalışılmıştır. Karşılaştırmalar, mikroscopik benzeşim sonuçları baz alınarak yapılmıştır.

Anahtar Kelimeler: İyon kanalı, Kanal gürültüsü, Stokastik Hodgkin-Huxley, Markov zinciri, Minimal difüzyon formülasyonu.

ACKNOWLEDGMENT

I would like to acknowledge and express gratitude Prof. Dr. Marifi Güler. This research would have seen impossible without the guidance, knowledge, and experience that he provided.

I am also very grateful to everyone who helped me. I deeply acknowledge to my family for they are always supporting and helping me. I love you all.

TABLE OF CONTENTS

LIST OF TABLES

LIST OF FIGURES

LIST OF SYMBOLS AND ABBREVIATIONS

Diffusion Approximation	DA
DSM	Dissipative Stochastic Mechanics
HH	Hodgkin-Huxley
K	Potassium
MC_S	Markov Chains
MD	Minimal Diffusion
Na	Sodium
NCCP	Nontrivial Cross-Correlation Persistency
PSP	Postsynaptic Potential
SNR	Signal-to-noise Ratio
SR	Stochastic Resonance

Chapter 1

INTRODUCTION

The excitability of cells, as an essential physiological process, entails the process through which voltage-gated ion channels enable the conductance of potassium and sodium, as well as the numerous gates accommodated in each of the individual ion channels. In response to Hille (2001)'s charge that it was necessary to explore the impact that gate multiplicity has on the functioning of a cell, particularly when the size of the membrane is limited. Furthermore, bearing in mind a realistic membrane, (Güler, 2011) found that gate multiplicity had a significant character to play in the performance of a limited-size of cell as it led to nontrivially tenacious membranous cross correlations(NCCP). NCCP seemingly the primary reason for the increased excitability and spontaneous firing in small neuronal membranes.

The impact of noise on the neurons results in an abnormal configuration of the neuronal dynamic. The noise may be either internal or external (Faisal, 2008). The limited numbers of voltage gated ion channels are the foremost source of internal noise in a neuronal membrane spot. These channels can usually be found in either of two states: open or closed. The amount of channels when opening oscillates of a seemingly unsystematic manner Sakmann and Neher (1995) leading to the conclusion that that there is a fluctuation in the level of conductivity of the membrane itself thus implying variations in the transmembrane voltage.

Zeng and Jung (2004) explored the place of synaptic noise in the creation of action potentials by small and large clusters of ion channels within the neuronal membrane; the voltage dynamic is represented by Hodgkin-Huxley (1952)'s renowned equations when there is a large number of ion channels. However, a smaller membrane patches, the potential of influence on the voltage activity of the cell caused by fluctuations in the channel are potentially overwhelming (Güler, 2013a). Furthermore, the nontrivial cross correlation persistency (NCCP) increases the consistency of the spike train; the normalization of which is to be realized through the incorporation of appropriate functional procedures in the deterministic of equations.

Correspondingly, more reliable and overt route would be to introduce the colored noise sketch in the excitable membrane (Güler, 2013a). For this purpose, the term of a Gaussian White noise exists of the Langevin equation in each individual gating variable as in Fox & Lu (1994)'s equations and additional term of colored noise available of the conductance. Within the context of, Kurtz (1978) approximated the Markov process, which is dependent on density, through a series of stochastic differential equations (Baxendale, 2011) in a study of ion channel clusters (Fox and Lu, 1994).

Numerous studies have investigated the role of channel noise in causing unprompted firing in regularly uneventful membrane patches (DeFelece and Isaac, 1992; Strassberg and DeFelece, 1993; Rowt and Elson, 2004; Güler, 2007; Güler, 2008). Noise on the ion channels usually results in spontaneous fire though the generation of noise-induced action potentially varies as a result of analytical and numerical fluctuations in ion channels (Koch, 1999; White, 1998). Almassian and Güler (2011) discovered that a substantially greater SNR value was the result of the renormalized

equations of activity; a display of the Stochastic Resonance phenomenon occurred as a result (Jung and Shuai, 2001). While the inferiority of deterministic models relative to the DSM model has already been established (Güler, 2008), stochastic models (which exclusively use stochastic differential equations acquired through the insertion of some white-noise vis-à-vis vanishing) have also been known to result in lower SNR relative to the DSM model.

The level of requisite noise terms rises relative to the state space size, leading to the introduction of contemporary attempts at bypassing the matrix square root calculations (Orio and Soudry, 2012; Mélykúti, Kay, and Burrage, 2010). The preexisting model allowed for a particularly large number of noise terms and differential equations. (Zeng and Jung, 2004) provides a comparative overview of the aforementioned models in regards to their respective computation times as well as the model in paper (Güler, 2013b). The diffusion approximation formula is minimalistic, as it employs just two of stochastic variables equivalent to only two terms of noise despite of the density of the transition matrix and is hardly have been limited by the matrix square root operation. Even though, this is achieved by taking the consequences of fluctuations in the state density (less the density of the pertinent state) collectively, as opposed to taking said fluctuations individually. Employing this method in regards to ion channel cluster gating exemplifies its precision in replicating the numerical characteristics of the precise microscope Markov simulations. (Schmandt and Galan, 2012) argue that if fluctuations in only those states with a direct connection to the pertinent state of all chains are considered, the time needed to calculate the precise microscopic Markov simulations will be significantly reduced without only a negligible reduction in accuracy. Other diffusion models do not require a matrix square root computation (Orio and Soudry, 2012; Güler, 2013b; Linaro, 2011). Furthermore, the value of

parameters as well as the noise of variance during formulation is confirmed exclusively on the basis of criteria set forth in order to be portrayed by any reliable approximation sketch (Güler, 2015).

The gating of ion channels however, is usually cast by a Markovian kinetic sketch where transitions in the stochastic state are wholly dependent on the voltage in the membrane without any mention of particular molecular details (Sakmann and Neher, 1995; Hille, 2001). If we assume a two-state ion channel specification (open or closed), Markovian transitions may be depicted on the basis of the respective *residence time probability distributions* of remaining in both states. However, a multiexponential function is the autocorrelation function for single-channel conductance if we assumed a multistate ion channel specification (one open and at least two closed states) (Güler, 2007). It has been determined that the time distribution in the closed state residence is in fact, not exponential; this was revealed using the patch clamp technique, which allows individual ion channels to be used in calculating ionic currents, for experimental investigation (Sakmann and Neher, 1995).

The autocorrelation function is present in two exponentially decay additive terms. The formula posited by Güler includes variations of the marginal diffusion formulation and denotes the variants as two stochastic variables and one noise term (2v1n) and one stochastic variable and one noise term (1v1n); the two variants it has one noise. In recollection of the fact that the minimal diffusion formulation comprises a couple of stochastic variables and two noise terms, it is represented by the expression "2v2n model" otherwise "2v2n formulation" (Güler, 2016).

1.1 Structure of Thesis

This thesis is structured as follows: Chapter one provides a description of and introduction to the thesis. The second chapter gives a description of structure of neurons. Chapter three provides a description of ion channel dynamics. Chapter four describes the neuron models (Güler models (original minimal diffusion (2v2n)) and minimal diffusion with variant 2v1n, and 1v1n), Chapter five will describe minimal diffusion formulation. Chapter six shows the experiment and results, while Chapter seven is conclusion.

Chapter 2

STRUCTURE OF NEURONS

2.1 Introduction

Contemporary research into neural computation is driven to a large extent by a desire to invent artificial computing networks. However, as implied by the term 'neural network', the original objective of the field was to create modelling networks based on actual neural networks in the brain.

2.2 Neurons

Approximately 10^{11} neurons (nerve cells) of various kinds can be found in the brain. Figure 2.1 provides a schematic representation of the characteristics of a single neuron. The cell body or soma (the location of the cell nucleus) is connected to the dendrites (tree-like nerve fiber networks). A single long fiber, the axon, extends from the cell body and arborizes into various strands and substrands, at the ends of which are synapses – the transmitting ends of synaptic junctions, at their ends (Hertz and Palmer, 1991).

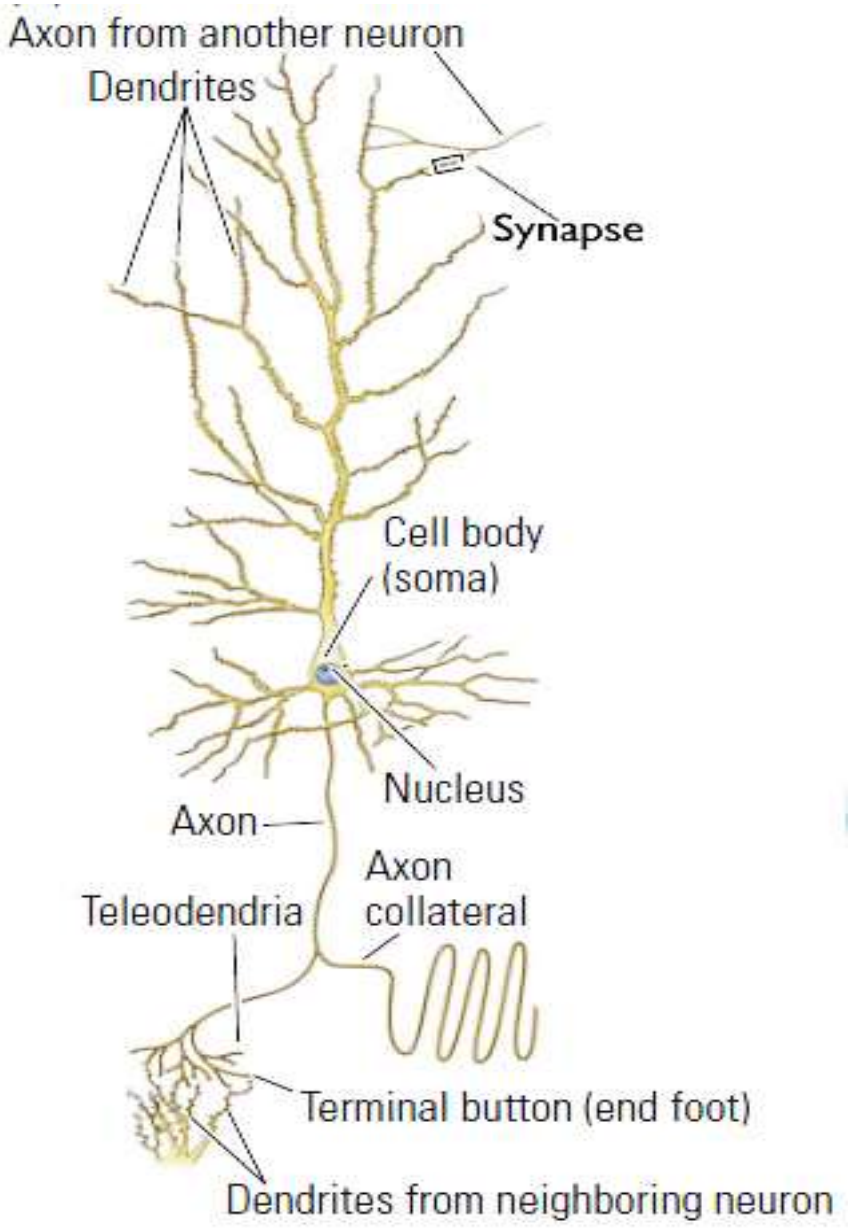

Figure 2.1: A drawing of the neuron highlighting its dendrites, cell body, and axon (Kolb and Whishaw, 2009).

The external and internal elements of a neuron are shown above in Figure 2.1 above. Largely responsible for increasing the neuron's surface area, the dendrites are arguably its most characteristic feature. Numerous branches and small protrusions known as *dendritic spines* cover every individual branch and further increase the surface area of the dendrite. A single neuron can have between one and twenty dendrites, each with at least one branch of its own; each individual branch has spines that can number in

the thousands. The surface area of the dendrites determines the amount of information the neuron can gather since it is the dendrites that collect information from other cells. Individual neurons have a single axon extending from the cell body. The terminal button at the end of this axon lies close to, but does not touch, the dendritic spine of another neuron. This 'almost connection' between the surface of the end foot of the axon, the matching side of the neighboring dendritic spine, and the gap between them is known as a *synapse*. Compared to the broad capacity of the dendrites and spines to gather information, the neuron's single axon limits it to only one communication output channel (Kolb and Whishaw, 2009).

2.2.1 Synapses

The connection between a presynaptic neuron's axon and a postsynaptic cell's dendrite (soma) occurs in a synapse. The chemical synapse is the most common type of synapse in the vertebrate brain. Here, the axon terminal lies pretty close to the postsynaptic neuron, resulting in a synaptic cleft: the little space left between the pre and post-synaptic cell membranes.

Thus far, two kinds of ion channels have been encountered: calcium activated ion channels and voltage activated ion channels. Transmitter-activated ion channels are a third type of ion channel participated in synaptic transmission with which we have to deal. Neurotransmitters are released into the synaptic cleft as a result of the activation of the presynaptic neuron. This caused the transmitter molecules to move to the opposite side of the cleft and cause receptors found in the postsynaptic membrane to be activated.

2.3 The Gate

The closing of a gate can interrupt the conduction of ion through the pore. Similarly, changes in temperature can also cause the gate to open and close sporadically, as well as a cause unwanted interruptions in the current. P_0, which is the probability that the gate is open in voltage-dependent channels, is contingent on the membrane potential. The P_0 in most voltage-dependent Na^+ , K^+ , and Ca^{2+} (Callahan and Korn,1994) channels from nerves and muscles rises relative to membrane depolarization (i.e. a decrease in the resting potential). There have been few instances where P_0 increases on hyperpolarization. One such instance is the Kat1 channel (Chung, Anderson, and Krishnamurthy, 2007).

2.4 Neuronal Dynamics

An intercellular electrode can be used to record the effect of a spike on the postsynaptic neuron. The intercellular electrode calculates the membrane potential: the likely difference between the cell's interior and its corresponding surroundings.

2.4.1 Spike

The short electrical pulses contained in neuronal signals can be observed through the placement of a fine electrode in the proximity of the soma or axon of a neuron. These pulses are also known as action potential or spikes (Gerstner and Werner, 2002).

Numerous types of cells, such as cells from pumpkin stems, eggs, and tadpole skin, have been known to produce voltage spikes across their cell membranes. Furthermore, *action potential* might be irrelevant for cell-to-cell signaling despite its role in cell division (Izhikevich, 2000).

The contacts on a typical neuron's dendritic tree are called synapses. These synapses allow the neuron to receive inputs from over ten-thousand other neurons (see Figure

2.1) and also change the membrane potential of the neuron by producing electrical transmembrane currents. While large currents result in significant postsynaptic potentials (PSPs) that the voltage-sensitive channels incorporated into the neuronal membrane can amplify and consequently result in a spike or an action potential, smaller channels produce only minimal PSPs. The spikes that result from large currents are the primary means of communication for the neurons; neurons hardly ever fire on their own and typically do so in response to spikes received from other neurons. Neurons aggregate all of the incoming PSPs and compare the "integrated" PSP with a voltage value. This value is known as the firing threshold. When the integrated value falls below the threshold, the neuron becomes dormant. However, it fires an all-or-none spike and restores its membrane potential to its original state when the integrated value moves above the threshold. Theoretical plausibility is added to this argument by referring to the Hodgkin-Huxley model of spike generation in squid (Izhikevich, 2007).

2.4.2 Bursting

Bursting occurs when neuron activity oscillates between repetitive spiking and a quiescent state (Izhikevich, 2000). Bursting is often the result of a slow voltage-dependent process capable of modulating fast-spiking activity. The underlying theory is based on the discovery that the dynamics of a neuron have numerous time scales and may be explained using a singular perturbed dynamical system (Izhikevich, & Hoppensteadt, 1997).

2.5 The Action Potential

Electrically stimulating the cell membrane at its resting potential results in concentrated graded potentials on the axon. Conversely, an action potential is a substantial, albeit brief, swap in the axon membrane's polarity with a duration of

approximately one millisecond. The sudden voltage reversal across the membrane in an action potential makes the interior of the membrane positive, relative to the exterior. That is, up until the voltage sharply reverses again and the resting potential is restored. This sudden change in polarity occurs when the membrane's potential depolarizes to threshold potential at approximately -50mV as a result of the large graded potential resulting from electrical stimulation. The membrane experiences significant change at -50mV, even without additional stimulation (Kolb and Whishaw, 2009).

Irrespective of the numerous mechanisms that facilitate the communication between neurons, action potentials still play a particularly crucial role. Because they involve sudden changes in a cell membrane's electrical potential, they can propagate in an essentially constant shape (Izhikevich, 2000). The neural axon is typically in either of two states. In the first, the results of processing in the soma are used as a basis for propagating an action potential. The shape and level of the propagating action potential are very stable, as is the possible difference across the cell membrane. This difference is reproduced at the axon's branching points. The amplitude is in the order of 10^{-1} mV. The axons do no propagate any action potential in the second (resting) state.

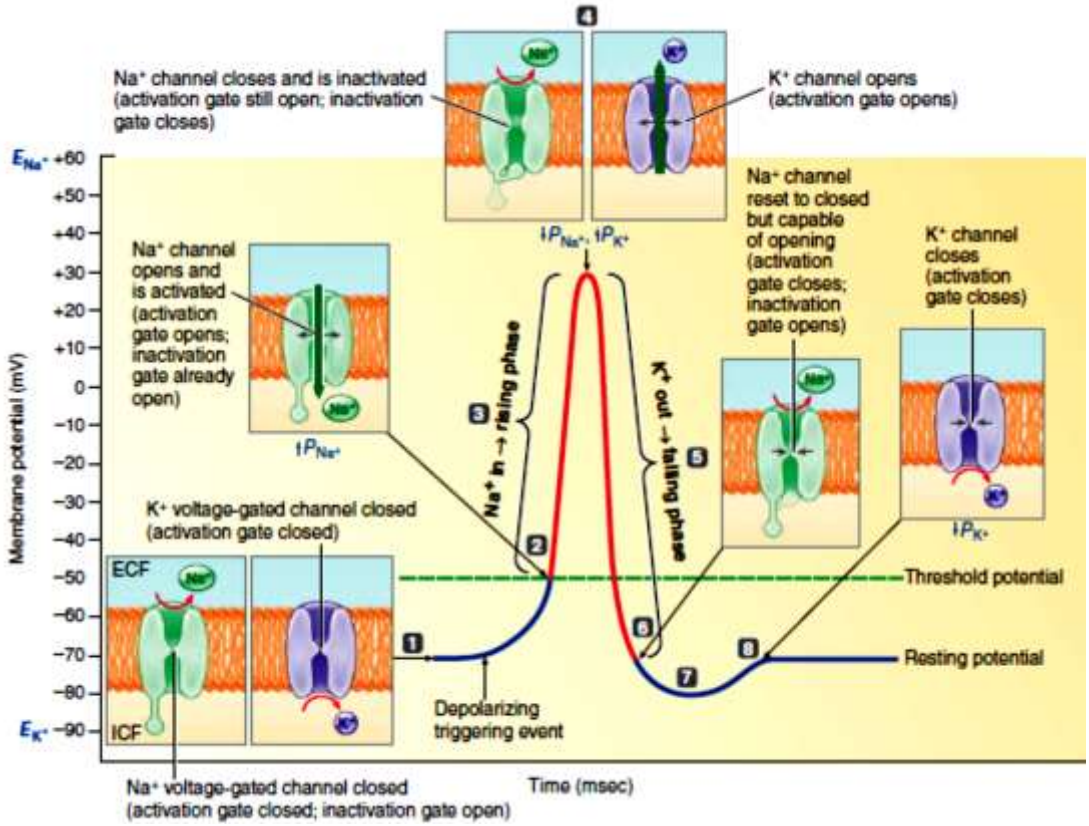

Figure 2.2: Permeability changes and ion fluxes during an action potential (Sherwood, 2011).

The above figure illustrates that (1) Resting potential: all voltage-gated channels closed. (2) At threshold, Na activation gate opens and P_{Na} rises. (3) Na enters cell, causing explosive depolarization. (4) At peak action potential, Na inactivation gate close and P_{Na} falls. At the same time, Kactivation gate opens at $P_k$rises. (5) K leaves cell, causing its repolarization resting potential, which generates falling phase of action potential. (6) On return to resting potential, Na activation gate closes and inactivation gate opens. (7) Further outwork movement of K through open K channel briefly hyperpolarizes membrane. (8) K activation gate closes, and membrane returns to resting potential.

2.6 Excitability

A ‘superthreshold’ input causes a large all-or-none action potential while a ‘subthreshold’ synaptic input results in a small graded postsynaptic potential in what is known as neuronal excitability. The neuronal excitability is larger than the sub-threshold response’s amplitude. Geometrically speaking, a dynamical system with a constant equilibrium is *excitable* when the large amplitude piece of trajectory is large and starts in a small area around said equilibrium, goes away from the area, and comes back to the equilibrium. These excitable systems occur close to bifurcations. A periodic trajectory may result from the modification of the vector field in the tiny shaded area.

2.6.1 Neuronal Excitability

While neurons are usually at rest, they are excitable in that they can react to certain stimuli by firing sparks. The computational properties of the neurons include: the spike latencies (delays), their firing frequency range, the coexistence of resting and spiking states, etc. From the perspective of dynamical systems, neurons alternate between spiking activity and resting and thus, are *excitable* due to their bifurcation. The computational properties of neurons are determined by the type of bifurcation, as opposed to the ionic currents (Inzikevich, 2007).

2.7 Noise in Spiking Neuron Models

In *vivo* recordings of the activities between neurons are often plagued with a high level of inconsistency. The irregularity of spikes in individual neurons is accompanied by the seemingly random relationship between the firing patterns of multiple neurons. One of the most pertinent problems facing neuroscience is how to uncover the rhythm behind the neuronal activity rather than just meaningless noise (Gerstner and Werner, 2002).

2.7.1 Spike Train

Neuron models, such as the Hodgkin-Huxley or the integrate-and-fire model, tend to produce a steady sequence of spikes when engendered by an equally steady and powerful current. Conversely, while neuronal models with adaptation currents might have constant inter-spike intervals, this is usually followed by an initial, short transient phase. The behavior of typical neuron spike trains in viva is considerably more irregular (Gerstner and Werner 2002).

2.7.2 Are Neurons Noisy?

A number of *in vivo* experiments have been known to demonstrate the noisy behavior of the central neuron. For instance, it is possible to record the activities of neurons in the visual cortex when a bar (moving slowly) is placed on screen in view of the animal under study (Gerstner and Werner, 2002). However, the spike train tends to fluctuate substantially between trials after several repetitions of the experiment. Additionally, the same neuron is also impulsively active. The intervals between subsequent spikes varies greatly during such spontaneous activity and causes the range of inter-spike intervals to be rather wide.

Is the presence of ubiquitous noise in the central nervous system proven by these experiments? The aforementioned observations relate to experiments that consider the neural system in its entirety. The cortical neuron that forms the field for such experiments receives inputs from numerous neurons in the brain in addition to those received from the retina.

2.7.3 Noise Sources

There are two types of noise sources: extrinsic noises, which are the result of network effects and synaptic transmission; and intrinsic noises, which generate stochastic behavior on the neuronal dynamic level (Manwani and Koch, 1999). Thermal noise is

literally an omnipresent source of noise. The voltage in any electrical resistor tends to oscillate at finite temperatures due to the discrete nature of electrical charge carriers (Johnson noise).

The neuronal membrane potential also fluctuates as a result of neuronal dynamics being represented by a similar resistor-containing electrical circuit. However, fluctuations resulting from Johnson noise are negligible in comparison to those cause by other sources of noise in neurons (Manwani and Koch, 1999).

The fixed number of ion channels in a neuronal membrane patch serve as another neuron-specific source of noise (White et al., 2000; Schneidman et al., 1998). These channels are always either open or closed.

2.8 Origins of computer science and neuroscience

Both Neuroscience and computer science came into being at nearly the same time and in influenced each other heavily in their formative stages. Over time, the fields have diverged excessively and have developed very different notions of seemingly shared concepts such as memory, cognition, and intelligence (Lytton, 2002).

One difference between the neuroscience and computer science viewpoints has to do through the necessary adoption of a big-picture approach through the computer scientists and a reductionist method by many neuroscientists. These two approaches are usually called top-down and bottom-up, respectively. The top-down approach rises from an engineering perspective: design a machine to do a particular assignment. If you're interested in intelligence, then design an artificial intelligence machine. The bottom-up perspective is the province of the phenomenologist or the taxonomist: collect data and organize it. Even granting that most U.S. science today is federally

mandated to be hypothesis-driven, a vital element of biology is the discovery of facts. Hypotheses are then intended to fit these facts together. As summarized here, these situations are caricatures. numerous biologists want to consider how the brain thinks, and several computer and cognitive scientists are interested in what roll on inside the skull.

Chapter 3

ION CHANNEL DYNAMICS

3.1 Introduction

Hodgkin and Huxley (1952) proposed a set of coupled, differential, nonlinear, deterministic equations, which is concerned with how sodium and potassium ions are conducted in the nerve membrane and the transmembrane voltage, which control how these ion currents are triggered. The transmembrane voltage is averse to metabolic energy, which is itself significantly affected by the ion currents. The governing rate constants depend on the particular voltage in question. These equations can, under specific conditions, result in solutions that display unstructured, yet periodic, spiking that is relatively similar to the calculated electrical voltage spiking in squid axon as has been observed by electrophysiologists

The patch-clamp technique posited by Neher and Sakmann (1995) has provided the opportunity to take certain measurements, which have shown that the minimalistic voltage fluctuations produced by individual ion channels are the result of said ion channels being simple stochastic elements that spontaneously open and close. A conclusion that was already considered based on previous voltage noise measurements but could not be confirmed as the measurements weren't for individual channels. It is almost certain that the origin of the ions' intrinsic stochasticity is thermal. DeFelice and Isaac (1993) integrated the ion channels' stochasticity in the computer model they used to microscopically describe the channel dynamics. Consequently, their model is

inherently stochastic as opposed to deterministic. It also uses the individual channels' voltage-dependent transition probabilities to indirectly couple them and possess an accelerated equilibration of the capacity of the transmembrane voltage in sizeable portions of the membrane.

3.2 Channel Noise

When variations are the result of seemingly random openings and closings of ionic channels, the result is channel noise. An ionic channel could either be a pore or a spore within a cell membrane. Ionic channel is so named based on the ionic species that it most commonly allows to pass through it – Na channel, K channel. Physically speaking, an ionic channel is understood to be a relatively big molecule, the different configurations of which match the channel being either closed or open; determined by a *gate*. Ionic channels noise is generally divided into one of two types: *nonsynaptic* and *synaptic* channels noise (Tuckwell, 1989).

3.2.1 Open Channel Fluctuations

Thermal fluctuations cause channels to remain in flux and constantly open and close. Consequently, the amount of open channels, and the amount of ion current permitted by said channels equally fluctuate. Let us first consider the channel transition starting from open and ends to close. For sodium channels every channel that is open has all 3 of its m-domains in an open state and its h-domain in a similarly open position. Should any of these cease to be open, the channel itself would close (Adair, 2003). According to HH, the depolarization happens when 3 of the domains, considered m, are typically closed at the membranes resting potential. The fourth, considered h, is mostly active at the resting potential and closes upon depolarization. Even though, the channel is considered open if the 3 similar m–domains are open and it has an active h domain, and is closed otherwise. When opening, Na ions permit into the cell driven through an

electrochemical gradient created through ion pumps. The K channel consists of 4 duplicate n-domains that are mainly in a closed state at the resting potential and drive to an open state on depolarization. Although, the channel is open while altogether domains are open and closed else. Thus, the potassium channels are same largely closed through the resting potential and then open while the membrane is depolarized permitting K ions to discharge motivated similarly by an electrochemical gradient. Nevertheless, the K channels open additional slowly than the sodium channels and also close slowly just happening repolarization.

3.3 The DSM Neuron

Güler (2006) first proposed utilizing stochastic mechanics, in occurrences of dissipation, as a means to model just how voltage dynamics in the excitable membrane were affected by ion channel noise. Güler (2007) further expanded the proposed ansatz-reliant method both in terms of its fundamentals and formalism. The present understanding of the prosed method is based on the latter paper. The unique formulation that mentioned in the DSM neuron s based on the understanding that conformational changes in ion channels are, in reality, exposed to two distinct types of noise. In the first, gates open and close based on different probabilities such that the voltage specifies the average (rather than precise) number of the gates open in the membrane. The movement of the voltage-dependent gating particles in and out of the membrane in this kind of noise is stochastic and is known as *intrinsic noise*. The other kind of noise, *topological noise*, results in the channels having more than one gate and thus, is inherently different from intrinsic noise. Topological noise is the result of changes in the topologies of open gates as opposed to changes in the amount of open gates. Due to their different origins, intrinsic and topological noises need to have their

effects on voltage dynamics formulated independently. Despite this, they both interact through the membrane voltage in a coupled form (Güler, 2007).

In a toy membrane with just 3 potassium channels (twelve gates), for example, 9 open gates may be set in various topological states with the possibility that either none, one, or two of the channels are open. Throughout the dynamics, the gating particles are hardly organized, both when leaving the open gates and occupying the closed gates that are available. As such, the membrane can have an identical number of open gates at two different times but with dissimilar conductance values. So, when regulating the voltage dynamics, all of the open gates' permissible topologies ought to be taken into consideration. The fluctuations resulting from the uncertainty surrounding access to acceptable topological states is known as topological noise, and motivates the implementation of stochastic mechanics. Two forms of noisy systems have been identified: the *collective* system and the *intrinsic* system. The former occurs in the membrane voltage phase space while the latter is the result of dynamical attributes linked with the gating particles. Understood to be under the influence of topological noise, the collective system is joined to the intrinsic system in a system–plus–reservoir strategy. While certain types of random noise can be found independently in both the collective and intrinsic systems, when they are not bothered by their respective existence, unpredictable effects are expected to result from the interaction between these two noisy systems. Consequently, reduced density operator techniques were used to calculate the voltage dynamics of the through the system (collective and intrinsic systems included). It has been discovered that the combination of both systems results in the renormalization of both the membrane capacitance and the voltage-dependent potential function, and channel dissipation (Güler, 2008).

3.3.1 The Approach for Signal-To-Noise Ratio Computation

One particular issue that results from extracting a signal from background noise is stochastic resonance (SR) (Adair, 2003). SR also coherently explains how weak signals are amplified in nonlinear systems. It is known that ion channel noise in neurons can result in stochastic resonance. While the actual optimal size of the cluster is contingent upon the frequency of the signal, it is usually either a large cluster size with several hundred or even thousands of channels or small clusters with only a few channels (Jung and Shuai, 2001). The stochastic resonance is typically determined using the ratio of the signal peak height to the height at the background – the signal-to-noise ratio (SNR). The aim of this study is to uncover the possible effects of renormalization terms on the SNR by way of periodic input currents. The following formula is used to measure SNR:

$$SNR = \frac{A_i}{CV\ (d)}$$

Where the amplitude of the input current is represented by A_i; $CV()$ represents the variation coefficient; d represents either the inter-bursting is the space among two consecutive bursts(time interval) during a bursting activity phase , or the inter-spike is the time between spikes (time interval). During a tonic firing activity phase. The variation coefficient the formula uses is defined as $CV(d) = \frac{Var(d)}{\mu}$, where $Var(d)$ is the variance of d, and μ is the average value of d. It was found that the renormalized correlations can lead to an increased SNR (Almassian and Guler, 2011b).

3.4 Application to Ion Channel Clusters

Specific types of ion channels conduct specific species of ions and control how channels conduct sodium and potassium through the membrane (Hille, 2001). The number of channels that are open at any specific point in time changes relatively

sporadically (Sakmann and Neher, 1995), causing both the membrane's conductivity and the transmembrane voltage to fluctuate. The fluctuations in the voltage are insignificant when the quantity of ion channels (which determines the area of the cell membrane) membrane patch is large. As such, the dynamics of the transmembrane voltage are described using the renowned Hodgkin-Huxley (HH) equations (Hodgkin and Huxley, 1952). The effects of channel fluctuations are possibly more intense, however, in smaller membrane patches. Figures 3.1 and 3.2 illustrates below the state transition figures for potassium and sodium respectively. As shown in the diagrams, sodium channels have 3 m gates and 1 h gate and potassium channel have 4 n gates (Chow and White, 1996).

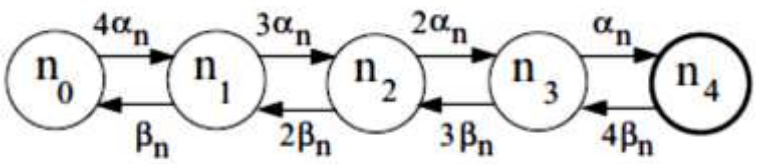

Figure 3.1: Kinetics scheme of state transition used for of a potassium channel (Chow & White, 1996).

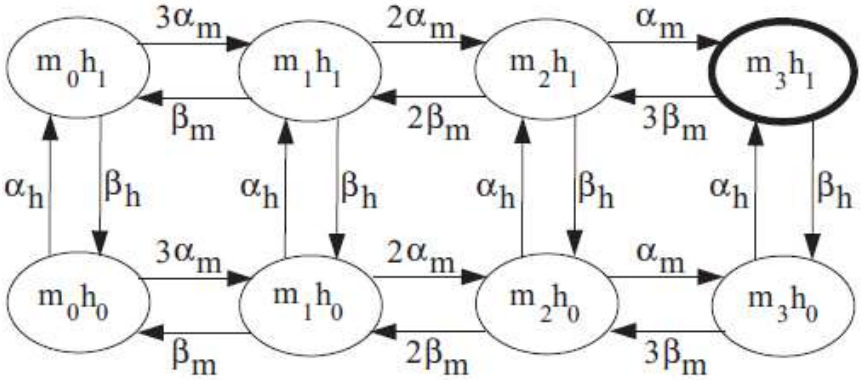

Figure 3.2: Kinetics scheme of state transition used for a sodium channel (Chow & White, 1996).

A channel is considered closed if at least one of its gates is closed. Furthermore, the individual channels do not interact with one another. The present formulation is easily

applied to potassium and sodium channel clusters by means of the state transition diagrams shown in Figures 3.1 and 4.1.

A basic stochastic approach that simultaneously monitors the Markov process for each gate can be used to provide a microscopic Markov simulation for a given channel population. There is a growing need to develop a different formulation in which the microscopic dynamics are competently approximated without a corresponding rise in the cost of computation due to increases in population size. In a seminal study, Fox and Lu (1994) investigated a method of diffusion approximation for discrete gate dynamics, where the vector including the fractions of likely channel states experiences changes corresponding to the Langevin-type of equation in matrix formula. Additionally, numerically calculating the square-root of matrix at every time step is required by this approach.

Chapter 4

MODELS OF NEURONS

4.1 The Hodgkin-Huxley Model

Through experiments performed on the giant axon of a squid, Hodgkin and Huxley (1952) discovered a leak current consisting primarily of cl^{-} ions and three kinds of ion current: potassium, sodium,. Separate specific voltage-dependent ion channels regulate the flow of sodium and potassium ions through the cell membrane. The Hodgkin-Huxley model's dynamics vary for different inputs – step current, pulse, and constant – and also take into account inputs dependent on time (Gerstner and Werner, 2002). In addition to functioning as a capacitor, the semi-permeable cell membrane also acts as a divide between the extracellular liquid that surrounds the cell and its interior. Injecting an input current into the cell can either lead to the presence of more charges in the capacitor, or even cause the current to permeate the cell membrane. The level of ion concentration in the cell's interior differs from the ion concentration in the extracellular liquid due to the movement of ion through the cell membrane. Batteries are a manifestation of the Nernst potential that results from the different levels of ion concentration.

4.2 The Membrane Dynamics

V, which represents the transmembrane voltage, evolves as such:

$$C\frac{dV}{dt} = -g_K\psi_K\,(V - E_K) - g_{Na}\psi_{Na}\,(V - E_{Na}) - g_L\,(V - E_L) + I \qquad (4.1)$$

Where the number of potassium channels were open relative to the aggregate number of membrane potassium channels is represented by variable ψ_K and the number of sodium channels were open is represented by ψ_{Na}. The value of the constant membrane parameters utilized in Eq. (4.1) are provided in Table 1. The equations of Hodgkin-Huxley (HH) approximate the channel variables ψ_K and the channel variable ψ_{Na} to the deterministic values $\psi_K = n^4$ and $\psi_{Na} = m^3h$; these values are representative of both the 4 n-gates present in a single potassium channel, and the single h-gate and 3 m-gates in a sodium channel. For a channel to be considered open, all of its constitutive gates must be open. Here, the gating variables are represented by *n*, *m*, *h*, the total number of K and Na channels are represented by N_K and, N_{Na} respectively, and the number of open h-gates, m-gates, and n-gates, correspond to $N_{Na}h$, $3N_{Na}$m, and $4N_Kn$.

Table 4.1: Instant of membrane (Hodgkin and Huxley, 1952)

C	Membrane Capacitance	$\mathbf{1\mu F/\ cm^2}$
$\boldsymbol{g_k}$	Maximal Potassium Conductance	36 mS/cm^2
$\boldsymbol{E_k}$	Potassium Reversal Potential	-12mV
$\boldsymbol{g_{Na}}$	Maximal Sodium Conductance	120mS/cm^2
$\boldsymbol{E_{Na}}$	Sodium Reversal Potential	115mV
$\boldsymbol{g_L}$	Leakage Conductance	0.3mS/cm^2
$\boldsymbol{E_L}$	Leakage Reversal Potential	10.6mV
	Density of Potassium Channels	18chns/μm^2
	Density of Sodium Channels	60chns/μm^2

The Markov process outlined below can also be used in computing gate dynamics. If one of the n-gates is closed at a specific time (t), $\exp(-\alpha_n \Delta t)$represents the probability of it being closed at time $t + \Delta t$, while $\exp(-\beta_n \Delta t)$represents the chance of it being open at time $t + \Delta t$. The opening and closing rates of n-gates, which are voltage-dependent, are denoted by the parameters α_n and β_n – similar for the rates of h-gates and m-gates. The rate function that is used therefore, is represented as:

$$\alpha_n = (0.1 - 0.01\,V)/(\exp(1 - 0.1\,V) - 1), \tag{4.2a}$$

$$\beta_n = 0.125\exp(-V/80), \tag{4.2b}$$

$$\alpha_m = (2.5 - 0.1\,V)/(\exp(2.5 - 0.1\,V) - 1), \tag{4.2c}$$

$$\beta_m = 4\exp(-V/18), \tag{4.2d}$$

$$\alpha_h = 0.07\exp(-V/20), \tag{4.2e}$$

$$\beta_h = 1/(\exp(3 - 0.1\,V) + 1), \tag{4.2f}$$

4.2.1 Conductance Fluctuations

Thus far, we have taken the sources of noise to have a passive path that matches the excitable element itself. To the end of gaining more intricate knowledge of the various processes within the membrane, the noise that results from the voltage-dependent conductance of Sodium (Na), specifically its fluctuations, becomes all the more interesting. For example, Lecar & Nossal (1971) analyzed how each conductance noise contributes to the overall fluctuations in the threshold. In particular, they searched for a model to account for how unitary conducting channels open and close, thus resulting in conductance noise.

Furthermore, Lecar & Nossal (1971) think through a model in which the voltage-dependent conductance originates from a Langevin force connected with thermal fluctuations of the amount of open channels. The equilibrium characteristics of the channel fluctuations be able to achieve in a common manner by a straightforward statistical argument. They characterize the normalized conductance, while channel is open and close. The average value equal to the probability that opening at the n-th times. Subsequently whole channels are identical and independent, the probability of every time are opening channel is in turn set by the expectation value, membrane conductance are normalized.

4.3 The Non-Trivial Cross Correlation Persistency (NCCP)

Knowing the number of open gates in a potassium channel (n) does not uniquely specify ψ_K since the channel has over one n-gate. To illustrate, while a toy membrane with eight gates in two potassium channels might have two open gates in one channel and four open in the other at time t_2; it can also have both channels each have three gates open at another time t_1. And so, while the total number of gates open at both times t_2 and t_1 is equal, one of the channels is open in the former, while none of them is open in the latter (see Figure. 4.1). Figure 4.1 (below) shows two conformational conditions of a figure membrane, at times $t_1$and t_2. The membrane consists of two potassium channels for a total of eight n-gates. The filled black circles represent open gates, while the small dots closed gates. The channels are represented by the larger circles. Regardless of the fact that at $t_1$and t_2 the number of open gates is the same (six), there is one open channel (shadowed) at t_2 and no channel is open at t_1- the gate-to-channel uncertainty. The terms *gate-to-channel uncertainty* and *gate noise* are respectively used to describe the uncertainty that occurs in regards to ψ_K even when the value for *n* has been computed, and the amount of fluctuations in *n*. Other terms

had hitherto been used to represent these two phenomena, but were changed following a conviction in the field that earlier terms did not convey as much clarity. The uncertainty regarding the gate-to-channel ratio manifests itself as a random dynamic variation in the construct $\psi_K - [\psi_K]$, which isolates the fluctuations in the channel that result from the uncertainty in the gate–to–channel ratio. Consequently, the construct would cease to exist if this uncertainty is to be resolved, regardless of gate noise.

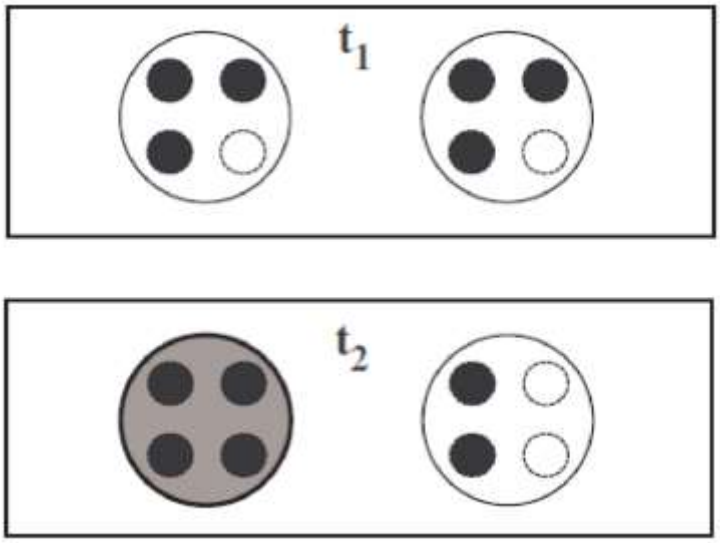

Figure 4.1: Two possible conformational states of a toy membrane (Güler, 2011).

In the above, the configuration average of the relative number of opening potassium channels is represented by ψ_K and is calculated for the membrane's possible $4N_K n$ open n-gates. The construct $\psi_K - [\psi_K]$ is used to calculate the difference between the configuration average at a particular point in time and the number of open channels. So long as the membrane is not too small, it is assumed that

$$\psi_K \approx n^4 \tag{4.3}$$

Güler (2011) found that $\psi_K - [\psi_K]$ (construct fluctuations) and the fluctuations of voltage in the phase of sub–threshold activity share a non-transient correlation, which

is precisely what is referred to by NCCP. The autocorrelation time of the construct $\psi_K - [\psi_K]$, while finite, must not equal zero; this is crucial for the occurrence of NCCP. Looking at Equation 4.1, it is evident that a negative variation comparable to $\psi_K - [\psi_K] > 0$ happens in V over a particular period in time. Conversely, the variation is positive if throughout $\psi_K - [\psi_K] < 0$ in the same period. NCCP occurs so long as the residence time for $\psi_K - [\psi_K]$ is of a suitable duration in the algebraic sign. A pictorial illustration is offered in Figure 4.2.

According to the construct, the formulation $\psi_{Na} - [\psi_{Na}]$ is believed to represent the *gate–to–channel uncertainty* that accompanies to sodium channels. Provided the membrane is not extremely small, the configuration average of the number of sodium channels that are open $[\psi_{Na}]$ goes thus:

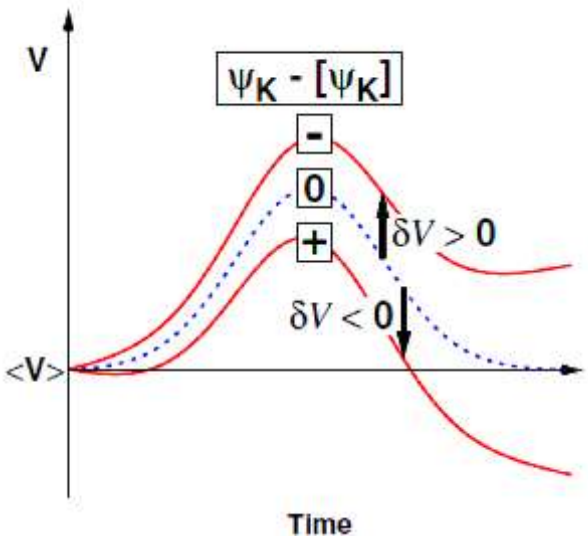

Figure 4.2: An illustration of the variant in the V. Adopted from Güler (2011).

$$\psi_{Na} \approx m^3 h \tag{4.4}$$

4.4 The Colored Noise Model Formulation

Because the autocorrelation time for $\psi_K - [\psi_K]$, is non-zero and (on a microscopic timescale) its algebraic sign is durable, ψ_K can be computed as

$$\psi_K = [\psi_K] + \mathcal{Q}_K \tag{4.5}$$

Where the autocorrelation time for $\mathcal{Q}_K$ – a stochastic variable with an expectation value equal to zero at equilibrium – is greater than zero. As such, it is possible to treat $\mathcal{Q}_K$ as colored noise. It is somewhat necessary, however, to properly define $\mathcal{Q}_K$ so as to analytically implement NCCP.

It is easier to approximating the equation 4.5 as:

$$\psi_K = n^4 + \sigma_K \mathfrak{q}_K \tag{4.6}$$

Where the approximation found in equation 4.3 was used, and a different stochastic variable – σ_K – is introduced. σ_K represents the standard deviation for ψ_K, which is calculated for the potential formations of a membrane with $4N_K n$ open n–gates. However, it is more convenient to calculate the standard deviation in a case whereby the probability of *n* covers the chance of each gate in each configuration being open without the limitation of being equal to $4N_K n$ open gates per configuration, is much easier. The following formula is applicable for such a case:

$$\sigma_K = \sqrt{\frac{n^4(1 - n^4)}{N_K}} \tag{4.7}$$

The formula for the random walk problem was only used in the above derivation of σ_K, after n^4 had been taken to represent the probability that a channel will be open. Güler (2013a) posited that, as represented in Equation 4.7, σ_K is a suitable estimate of the real standard deviation, although just for a proportionality constant incorporated into $\mathfrak{q}_K$. It is noteworthy that σ_K disappears in the bounded of an infinite membrane–size; consequently, the following formula is relevant for said limit: $\psi_K =$

n^4. No gate–to–channel uncertainty exists in regards to when all of the n–gates potassium channels are closed or open i.e. *n* = 0 or *n* = 1 respectively. As such, such cases are expected to be accompanied by the disappearance of colored noise and σ_K being equal to zero at these unique *n*-values.

Güler (2013a) considers the stochastic variable q_K to follow equations similar to those adhered to by the position variable of a *Brownian harmonic oscillator*. As a result, q_K demonstrates near periodicity, has memory, contains an unbounded variance and is stochastic. These are also the characteristics of the construct ψ_K — $[\psi_K]$ with a time of autocorrelation is nonzero. It is for this reason that we adopt the Brownian harmonic oscillator as a possible way to biologically emulate the construct. The dynamics of q_K are described by the following equations:

$$\tau \dot{q_k} = p_k \tag{4.8a}$$

$$\tau \dot{p_k} = -\gamma_k p_k - \omega_k^2 D_n q_k + \xi_k \tag{4.8b}$$

Where D_n is represented as

$$D_n := \alpha_n(1-n) + \beta_n n \tag{4.9}$$

And ξ_k is a zero–mean Gaussian white noise term with a mean square calculated as:

$$\langle \xi_k(t)\xi_k(t')\rangle = \gamma_K T_K D_n \delta(t-t') \tag{4.10}$$

τ is the parameter that equal to the unit time. Both the constants γ_K, ω_K and T_K, and the variables q_K and p_K are represented by dimensionless units. The speed at which a conformational state experiences memory loss (on a microscopic timescale) is represented by D_n. As α_n increases, so does an n–gate is the probability of transitioning from when closed to open; the probability of the gate transitioning from open to closed rises with β_n. q_K is expected to switch sign more frequently and behave more erratically when D_n is a larger value, thus causing it to be accompanied by the

constants ω_K and T_k. The proportionality of D_n to the noise variance which the n–gates in the FL equations is no coincidence. Based on non-equilibrium statistical mechanics (Zwanzig, 2001), it is assumed that if q_K obeys the above equations, its variance at equilibrium, is computed as:

$$\langle q_K^2 \rangle_{eq} = \frac{T_K}{\omega_K^2} \tag{4.11}$$

It is worth pointing out that the variance is, as it should be, a constant.

As was noted in the construct of $\psi_K - [\psi_K]$, the construct $\psi_{Na} — [\psi_{Na}]$ equally has a fixed autocorrelation time is non–zero that causes the NCCP characteristic of the sodium channels. Thus, the colored formulation intended for the K conductances able to be adapted for Na conductances. Applying approximation 4.4, were calculated ψ_{Na} using equation 4.6 as:

$$\psi_{Na} = m^3 h + \sigma_{Na} q_{Na} \tag{4.12}$$

Where q_{Na} is a stochastic variable with an autocorrelation time greater than 0 and a zero–expectation value at equilibrium. The standard deviation of ψ_{Na} is represented by σ_{Na}, which is calculated for all possible configurations of a membrane with $3N_{Na}m$ open m–gates and $N_{Na}h$ open h–gates. The method utilized in calculating σ_K may also be used for σ_{Na}; hence,

$$\sigma_{Na} = \sqrt{\frac{m^3(1-m^3)}{N_{Na}}\, h} \tag{4.13}$$

Both q_K and the stochastic variable q_{Na} adhere to the same kind of dynamical equations:

$$\tau \dot{q_{Na}} = p_{Na}, \tag{4.14a}$$

$$\tau \dot{p_{Na}} = -\gamma_{Na} p_{Na} - \omega_{Na}^2 D_m q_{Na} + \xi_{Na} \tag{4.14b}$$

Where D_m is denoted as

$$D_m := \alpha_m(1-m) + \beta_m m \tag{4.15}$$

The Gaussian white noise term ξ_k has a zero-mean and a mean square denoted as:

$$\langle \xi_{Na}(t)\xi_{Na}(t')\rangle = \gamma_{Na}T_{Na}D_m\delta(t-t') \tag{4.16}$$

At equilibrium, the variance of q_{Na} is:

$$\langle q_{Na}^2\rangle_{eq} = \frac{T_{Na}}{\omega_{Na}^2} \tag{4.17}$$

The table 4.2 includes the constant value of The above variable are given by:

Table 4.2: The values of parameters

$\gamma_K = 10$	$\omega_K^2 = 150$	$T_K = 400$
$\gamma_{Na} = 10$	$\omega_{Na}^2 = 200$	$T_{Na} = 800$

4.5 The Gate Noise

In addition to providing a better understanding of NCCP, the whole set of analytical activity should also account for the gate noise. For this purpose, FL's Langevin equations were used as a reference point used for the gating variables. In the (Güler, 2011a) case, the white noise terms utilized in the Langevin–equations have changed noise variances. The following formulae apply to the gating variables:

$$\dot{n} = \alpha_n(1-n) - \beta_n n + \eta_n \tag{4.18a}$$

$$\dot{m} = \alpha_m(1-m) - \beta_m m + \eta_m \tag{4.18b}$$

$$\dot{h} = \alpha_h(1-h) - \beta_h h + \eta_h \tag{4.18c}$$

Where the mean zero Gaussian white noise terms η_n, η_m, and η_h are assumed to have mean squares computed as follows:

$$\langle \eta_n(t)\eta_n(t')\rangle = \frac{D_n}{4N_K}\delta(t-t') \tag{4.19a}$$

$$\langle \eta_m(t)\eta_m(t')\rangle = \frac{D_m}{3N_{Na}}\delta(t-t') \tag{4.19b}$$

$$\langle \eta_h(t)\eta_h(t')\rangle = \frac{D_h}{N_{Na}}\delta(t-t') \tag{4.19c}$$

The terms D_n and D_m were respectively defined in equations 4.9 and 4.15.

D_h is likewise defined as:

$$D_h := \alpha_h(1-h) + \beta_h h \tag{4.20}$$

Furthermore, the study also chooses to utilize the Brownian motions as opposed to the Gaussian white noise terms η_n, η_m, and η_h in equations 4.18a to 4.18c (Saarinen..., 2008). It does, however, still adopt the (Fox and Lu) formula for the gating variables as the formula was used in developing the white noise terms in the gating dynamics equations.

4.6 HH Model Under Noisy Rate Function

Study of dynamics under noisy rate functions is also of interest. In this context Güler (2013b) opines that the weak performance of the Linaro, Storace et al. The model in (Güler, 2011) is the result of its use of a covariance function of open channels at the steady state in its derivation. Conversely, the model (Güler, 2011b) does not succumb to the problem of noise being present in the rates since it does not utilize steady-state approximation as in the Linaro et al. model. This makes it a more generic formulation that is more reliable for mechanisms aimed at generating neuronal signal with unique specifications. Additionally, it has also been argued in the context of gating particles that the anticipated noise in the rate functions is possibly of a physiological nature. However, the stochasticity is generally uncommon and usually only affects smaller membrane sizes.

The noise terms in the conductances, ϕ_k^G and ϕ_{Na}^G, were also taken into consideration in an effort to gain a better understanding of NCCP. The two terms are functions of their attendant gating variables: ϕ_k^G depends on *n* while ϕ_{Na}^G depends on m and h. The NCCP characteristic of the potassium channels is represented by term ϕ_k^G , which is computed as:

$$\phi_k^G = \sqrt{\frac{n^4(1-n^4)}{N_K} q_K} \tag{4.21}$$

The following formula represents the NCCP attributed to the sodium channels:

$$\phi_{Na}^G = \sqrt{\frac{m^3(1-m^3)}{N_{Na}} h q_{Na}} \tag{4.22}$$

Where q_{Na} obeys a stochastic variable having a zero-mean Gaussian white noise. All of the pertinent values can be found in Güler (2013b); both the noise terms associated with the gating variables and their mean squares are Gaussian.

The values representing the variance of η_h in the present study are similar to that used in Fox and Lu (1994)'s model. However, the variances for both η_n and η_m are respectively one-fourth and one-third of their variances in the Fox and Lu model. Based on the non-equilibrium statistical mechanics, it can be concluded that the variances for the stochastic variables q_k and q_{Na} at equilibrium can be computed. During the numerical application of the model (Güler, 2011b), subsequent checks are necessary following every time step to ensure that the noise terms that in Equations 4.18a until 4.18c do not have a value other than 0 or 1 for either *n*, *m*, or *h*. If they do, the relevant step must be carried out again with a new set of numbers each for $\eta_n, \eta_m, or\ \eta_h$.

Chapter 5

MINIMAL DIFFUSION FORMULATION

Güler (2015) recently suggested that each of the ensemble's chains be imagined as a particle to make them easier to visualize. The formulation offers a diffusion approximation so as to determine the dynamics for the density of chains in a particular relevant state, and is valid after the system is relaxed. The ensemble is understood to be comprised of Markov chains of an ergodic (irreducible) Markov chain continuous-time nature, which autonomously evolve within a shared transition rate matrix in the limited spaces of certain states. The cardinal benefit of the formulation is that it is not too complex. Notwithstanding the size of the state space or density of the transition matrix, it is always comprised of only two noise terms and two stochastic variables, neither is it limited by matrix–square root operations. The formulation is allowed to function such that it takes the effects of state density fluctuations for non-relevant states as a collective as opposed to individually.

However, because it does not use any other state density fluctuations besides ϕ_r and ϕ_s – as the overall result of all other density fluctuations is inherent to the formulation (Güler, 2015) – the diffusion approximation advanced here does not suffer from the aforementioned problems. Furthermore, at equilibrium and characterized by the probability of transition, the process ϕ_s is Markovian process and also stationary process. It may also be taken as a Gaussian process, although this is not entirely accurate. In reality, it is actually an Ornstein-Uhlenbeck; this is the conclusion drawn

from Doob's theorem. When the process is concurrently stationary, Markovian process, and Gaussian process, it is either a entirely random process or an Ornstein-Uhlenbeck.

N is taken to represent how many Markov chains the ensemble has, while $\{0, \ldots L\}$ represents the space of the states. Additionally, θ_l ($l = 0, \ldots L$) denotes how many chains are in state *l* at a specific time, while the synonym is $\psi_l := \frac{\theta_l}{N}$ represents the state's density. The state density's fluctuation in the ψ_l is symbolized by θ_l; that is:

$$\psi_l := \frac{\theta_l}{N} \langle \psi_l \rangle + \phi_l$$

Where the expectation value is represented by ψ_l. It is worth mentioning that the chance of discovering a chain in state *l* is a probability correlates with the average state density $\langle \psi_l \rangle$. Essentially, this reads:

$$\sum_{l=0}^{L} \langle \psi_l \rangle = \sum_{l=0}^{L} \psi_l = 1 \tag{5.1}$$

$$\sum_{l=0}^{L} \phi_l = 0 \tag{5.2}$$

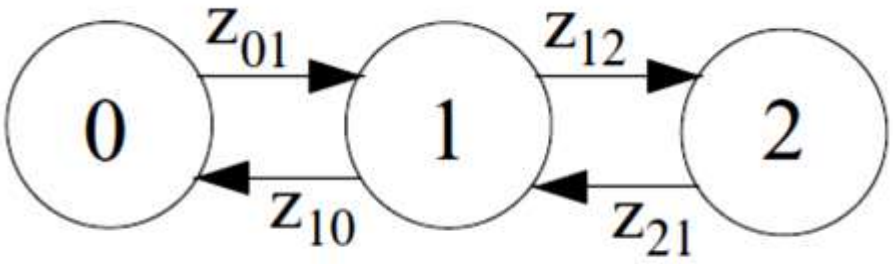

Figure 5.1: Case of a state transition diagram represented that the demonstration of the master equation (Guler, 2015).

A coupled linear deterministic differential equations is represented by The *L*, and then the master equation governs, can be used to calculate how the expectation values

evolve $\langle\psi_l\rangle$ (l = 0,1, . . ., L). One fundamental characteristic of the master equations in Markov processes is that every solution has a tendency to be stationary when the state set contains an explicitly limited amount of discrete states and the timing of the transition rates remains unchanged as $t \to \infty$. Consequently, when transition rates are constant, $\langle\psi_l\rangle$ (l = 0,1, . . ., L) attains a distinct constant state overtime. The minimal diffusion formulation will take transition rates to either experience very little change, or as constant. In the case of the illustrative state transition diagram in Figure 5.1, the master equation reads as:

$$\frac{d\langle\psi_0\rangle}{dt} = \mathcal{Z}_{01}\langle\psi_0\rangle + \mathcal{Z}_{10}\langle\psi_1\rangle$$

$$\frac{d\langle\psi_1\rangle}{dt} = \mathcal{Z}_{01}\langle\psi_0\rangle - (\mathcal{Z}_{10} + \mathcal{Z}_{12}\langle\psi_1\rangle + \mathcal{Z}_{21}\langle\psi_2\rangle \tag{5.3}$$

$$\frac{d\langle\psi_2\rangle}{dt} = \mathcal{Z}_{12}\langle\psi_1\rangle - \mathcal{Z}_{21}\langle\psi_2\rangle$$

And Eq. (5.2) becomes

$$\langle\psi_0\rangle + \langle\psi_1\rangle + \langle\psi_2\rangle = 1 \tag{5.4}$$

Depending on the constraint (5.4). For constant transition rates, the steady state

$$\frac{d\langle\psi_0\rangle}{dt} + \frac{d\langle\psi_1\rangle}{dt} + \frac{d\langle\psi_2\rangle}{dt} = 0 \tag{5.5}$$

Equations (5.3)–(5.5) uniquely solve $\langle\psi_0\rangle$, $\langle\psi_1\rangle$, and $\langle\psi_2\rangle$

5.1 The Fluctuations of the Relevant State Density

When the dynamics of the fluctuation is formulating ϕ_r – where the relevant state is denoted by the subscript r – the special case where r shared a direct connection with only one state (such as state s, shown below) is an appropriate starting point:

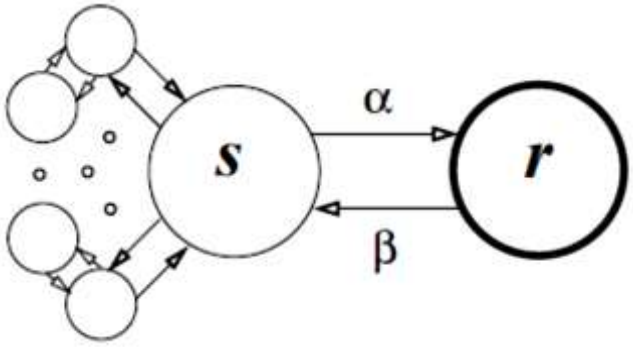

Figure 5.2: relevant state makes through connection with one state only (Güler, 2015).

Assuming that the transition rates shown in Figure. 5.2 (α and β) are positive constants and minimal diffusion formulation supposes an equilibrium context, although the equations below are outlined then adapted for the evolution of state density fluctuations and remain true after the system has relaxed.

The differential equations:

$$\dot{\phi}_r = -\beta\phi_r + \alpha\phi_s + \xi \tag{5.6a}$$

$$\dot{\phi}_s = -\gamma\phi_s - \xi + \eta \tag{5.6b}$$

Where the parameter γ is given as

$$\gamma = \frac{\alpha\langle\psi_s\rangle^2 + \beta\langle\psi_r\rangle(1 - \langle\psi_s\rangle)}{\langle\psi_s\rangle\langle\psi_r\rangle} \tag{5.7}$$

where the mean square mean of the zero Gaussian white noise ξ is:

$$\langle\xi(t)\xi(t')\rangle = \frac{\alpha\langle\psi_s\rangle + \beta\langle\psi_r\rangle}{N}\delta(t - t') \tag{5.8}$$

Calculating the square root of a matrix is necessary in the original description – in its general form for a Markov Chain (MC) with at least two states – of the diffusion approximation (DA) (Fox and Lu, 1994). Furthermore, Orio and Soudry (2012) found that it is more common for the proposed DA method to have a numerical stability

similar to that of MC modelling, even when the former uses a basic Euler-Maruyama integration scheme.

The terms ξ and η in Eq. (5.6a) and (5.6b) are autonomous zero mean Gaussian white noises, the mean squares of which are calculated using Eq. (5.8) and

$$\langle \eta(t)\eta(t') \rangle = \frac{\alpha\langle \psi_s \rangle C_\alpha + \beta\langle \psi_r \rangle C_\beta}{N} \delta(t - t') \tag{5.9}$$

The synonyms C_α and C_β in Eq. (5.9) are respectively calculated as follows:

$$C_\alpha := 2\langle \psi_s \rangle (1 - \langle \psi_s \rangle) - \psi_r \tag{5.10a}$$

$$C_\beta := 2(1 - \langle \psi_s \rangle)^2 - \langle \psi_r \rangle \tag{5.10b}$$

As such, in computing the relevant state density fluctuation ϕ_r from the aforementioned formulation through $\langle \psi_r \rangle$ (in the master equation), the evolution of ψ_r is calculated as:

$$\psi_r = \langle \psi_r \rangle + \phi_r$$

The stochastic differential Langevin equation is characterized by an Ornstein-Uhlenbeck process, and so Güler (2015) employed the following equation for the evolution of ϕ_s:

$$\dot{\phi_s} = -\gamma\phi_s - \xi + \eta \tag{5.11}$$

Where η is Gaussian white noise with mean zero autonomous from ξ. The $-\xi$ term in Equation 5.2 was added for the purpose of counter-balancing ξ 's influence on ϕ_s. The parameter γ and in the same time the variance of η were calculated in Güler (2015) by solving a differential equation, and are, for the progress of fluctuations in the state density, at equilibrium in the ensembles of Markov Chain.

5.2 Autocorrelation Function of the Relevant State Density in The Minimal Diffusion Formulation Model (2v2n Model)

Güler (2016) calculated the autocorrelation function for the relevant state's density in the 2v2n formulation. This calculation is relevant not just on the basis of its merit, but also because the autocorrelation function is the foundation of the 2v1n and 1v1n models. The calculation takes the transition rates to be constant and is especially relevant in the long-run.

The differential equations 5.6a and 5.6b are respectively used to calculate the values for ϕ_r and ϕ_s. While not absolutely essential, assuming that the system had already reached equilibrium at time 0 is somewhat helpful. Assuming that $\langle \eta\xi \rangle = 0$, and is read in the limit $t \longrightarrow \infty$, ϕ_s^2 is calculated as:

$$\langle \phi_s^2 \rangle = \frac{\langle \psi_s \rangle (1 - \langle \psi_s \rangle)}{N} \tag{5.12}$$

As transition rates are assumed to be time-independent in the present study, it is possible to incorporate the average state densities at the steady state found in Güler (2016)'s equation. The master equation for $\langle \psi_r \rangle$ is computed as:

$$\frac{d\langle \psi_r \rangle}{dt} = -\beta \langle \psi_r \rangle + \alpha \langle \psi_s \rangle \tag{5.13}$$

Which leads to the conclusion that

$$\alpha \langle \psi_s \rangle = \beta \langle \psi_r \rangle \tag{5.14}$$

at the steady state. And so, by incorporating Equation 5.14 into Equations 5.8, 5.9, and 5.12, we find that the inequality $\langle \psi_r \rangle + \langle \psi_s \rangle < 1$ is consistently finite and positive. The equation gives the variance:

$$\langle \phi_r^2 \rangle = \frac{\langle \psi_r \rangle (1 - \langle \psi_r \rangle)}{N} \tag{5.15}$$

It results of the binomial distribution of dissipation relation in agreement with that provided in Güler (2015).

The autocorrelation function of ϕ_r is given by (Güler, 2016) computing expected value $\langle\psi_r\rangle$ in equation 5.13 and where gives equation 5.14 steady state is released. After utilizing equation 5.14 in equation (5.7), (5.8) and (5.12) gives equation 5.16.

$$N\langle\phi_r(t)\phi_r(t+\tau)\rangle = \langle\psi_r\rangle\left(1-\frac{\langle\psi_r\rangle}{1-\frac{\alpha}{\beta}\langle\psi_r\rangle}\right)e^{-\beta\tau}+\frac{\beta\langle\psi_r\rangle^3}{\alpha-\beta\langle\psi_r\rangle}e^{-y\tau} \tag{5.16}$$

5.3 The Variant 2v1n

In contrast to the 2v2n formulation, which has two noise terms, the 2v1n formulation comprises of two stochastic variables and a single noise term. The two formulations do, however, have identical autocorrelation functions and standard deviations for relevant state density fluctuations.

The density fluctuation ϕ_r in this variant is calculated as:

$$\phi_r = k_a\phi_{r,a} + k_b\phi_{r,b} \tag{5.17}$$

Where k_a and k_b are specific parameters, and $\phi_{r,a}$ and $k_b\phi_{r,b}$ are two diffusively coupled Ornstein-Uhlenbeck calculated using the following Langevin equations:

$$\dot{\phi_{r,a}} = -\beta\phi_{r,a} + \xi \tag{5.18a}$$

$$\dot{\phi_{r,b}} = -\gamma\phi_{r,b} + \xi \tag{5.18b}$$

Here, the mean square of the zero-mean Gaussian white noise ξ is calculated using Equation (5.8). The parameters k_a and k_b are set such that they help in attaining an autocorrelation function matching that gotten using the 2v2n model. The specific parameters are calculated using the following formulae:

$$k_a = \sqrt{\frac{2\beta(\beta+\gamma)C_2}{2\beta C_3+\beta+\gamma}} \tag{5.19}$$

And

$$k_b = C_3 k_a \tag{5.20}$$

Where both the differential equations 5.18a and 5.18b, their respective solutions, and the coefficients of C_2 and C_3 are provided by Güler (2016).

The parity between the 2v1n and 2v2n formulations is not easily substantiated however, as they might still have different transition probability functions. Regardless, the congruence between their respective autocorrelation functions makes the 2v1n and 2v2n formulations extremely compatible when computing fluctuations in the state density.

5.4 The Variant 1v1n

An alternative formulation that is simpler than the 2v1n and 2v2n formulations is the 1v1n formulation. This formulation has only one stochastic variable and one noise term. Unfortunately, however, its relevant state autocorrelation function only matches up with that of the 2v2n formulation in the time gap's first order. The following Langevin equation denotes the diffusive dynamics for this formulation read as:

$$\dot{\phi}_r = -\tilde{\gamma}\phi_r + \xi \tag{5.21}$$

The same noise from Langiven type of equation here, ξ is a zero mean Gaussian, the mean square of which is computed through Equation 5.8, and parameter $\tilde{\gamma}$ is the friction coefficient has been calculated.

While the approach adopted by Linaro et al. (2011) is relevant for older Langevin-based formulations, it is considerably different in terms of how it reintroduces channel fluctuations in model equations. It is a precise and systematic generalization of the algorithm posited by Fox (1994) and provides analytical results detailing where it has failed as supporting information. On the other hand, a more effective method for

single-compartment neuronal simulations is to define the precise simulations of the stochastic channel's kinetic schemes. The occupation numbers of these simulations could have large fluctuations, thus resulting in larger noise levels. The simulated Markov chains used here (despite the size of the fluctuations) utilize the "stochastic-shielding" approximation posited by Schmandt and Galán (2012). The approximation is only appropriate for cases in which only a small sample of states in the model is relevant. To illustrate, in a case where the relevant state only connects directly to just one other state (Figure 5.2), the totality of fluctuations in all of the states disappears as:

$$\sum_{l=0}^{L} \phi_l = 0$$

Because all state density fluctuations apart from ϕ_r and ϕ_s are set to zero in the stochastic shielding approach, the result is that $\phi_s = -\phi_r$. As such, the diffusion approximation relative to the stochastic shielding simulation approach is given as:

$$\dot{\phi_r} = -(\alpha + \beta)\phi_r + \xi \tag{5.22}$$

Where the noise ξ is identical to that given in Equation 5.8. The minimal diffusion formula 5.6a can easily be used to deduce this stochastic differential equation. When compared to Equation 5.21, it is evident that the stochastic shielding diffusion and 1v1n formulation share a single differential equation within an identical noise variance, however here have different values for parameter $\tilde{\gamma}$. The variance at equilibrium can be computed using Equation 5.23 below:

$$\langle \phi_r^2 \rangle = \frac{\beta \langle \psi_r \rangle}{N(\alpha + \beta)} \tag{5.23}$$

This variance however, differs from the dispersion relation (5.15). It is for this reason that the 1v1n formulation has better accuracy than the stochastic shielding diffusion approximation in determining the autocorrelation function, at least for smaller time

gaps. Güler (2015) provides a discussion on stochastic shielding as it related to the minimal diffusion formulation.

Chapter 6

EXPERIMENTS AND RESULTS

6.1 Results Discussion

Applying the present formulation to sodium and potassium channel clusters is easily done via the state transition diagrams contained in Figures 3.1 and 3.2 in the third chapter.

Here, performing the calculations is a simple matter of using the average of each gating variable represented by $\overline{n}$, $\overline{m}$ and $\overline{h}$, rather than specifying ψ_r for ψ_s for each of the channel types through the master equation. The averages of each of the gating variables are calculated using the following formulae:

$$\dot{\overline{n}} = -\beta_n \overline{n} + \alpha_n(1 - \overline{n}) \tag{6.1a}$$

$$\dot{\overline{m}} = -\beta_m \overline{m} + \alpha_m(1 - \overline{n}) \tag{6.1b}$$

$$\dot{\overline{h}} = -\beta_h \overline{h} + \alpha_h(1 - \overline{h}) \tag{6.1c}$$

Where the opening and closing rates of *n* gates are respectively denoted by α_n and β_n; those for *m* gates are α_m and β_m; and $\alpha_h$and β_h for *h* gates. The following formulae therefore, are used for potassium channels:

$$\langle \psi_4 \rangle = \overline{n}^4 \tag{6.2a}$$

$$\langle \psi_3 \rangle = 4\overline{n}^3(1 - \overline{n}) \tag{6.2b}$$

While sodium channels are calculated using:

$$\langle \psi_{31} \rangle = \overline{m}^3\overline{h} \tag{6.3a}$$

$$\langle\psi_{21}\rangle = 3\overline{m}^2(1-\overline{m})\overline{h} \tag{6.3b}$$

$$\langle\psi_{21}\rangle = 3\overline{m}^2(1-\overline{m})\overline{h} \tag{6.3c}$$

Where the average chain densities of both channels' relevant states are respectively represented by $\langle\psi_4\rangle$ and $\langle\psi_{31}\rangle$. Because no other state shares a direct connection to either the sodium relevant state m_3h_1, or the potassium relevant state n_4 calculating the expectations values for other states is not necessary.

Here, *j* is the probability will open n–gates of a K channel is represented by $\langle\psi_j\rangle$ (*j* = 0, …,4), while the likelihood of the probability that *i* open for Na channel having m–gates and, *j* open *h* gates is denoted by $\langle\psi_{ij}\rangle$ (*i* = 0, 1, 2, 3; *j* = 0, 1).

Therefore, for a potassium channel cluster:

$$\alpha = \alpha_n, \beta = 4\beta_n, \langle\psi_s\rangle = \langle\psi_3\rangle,$$

By virtue of Eqs. (6.1a) and (6.2). Then, the density of ψ_4 open potassium channels is calculated as $\psi_4 = \langle\psi_4\rangle + \phi_r$. Before using the formulation, the equations in Güler's (2015) paper should be evaluated for sodium channel clusters using the following settings:

$$\beta = 3\beta_m + \beta_h, \alpha_j = \alpha_m, \alpha_k = \alpha_h,$$

$$\langle\psi_j\rangle = \langle\psi_{21}\rangle,\ \langle\psi_k\rangle = \langle\psi_{30}\rangle.$$

Which is easily followed by the density of open sodium channels $\langle\psi_{31}\rangle$.

Here, Eqs. (6.1b), (6.1c), and (6.3) are used to calculate for $\langle\psi_{31}\rangle$, $\langle\psi_{21}\rangle$, and $\langle\psi_{30}\rangle$. Depending on the particular channel type being considered, the parameter N denotes the amount of cluster in the potassium or sodium channels when using the formulation. A numerical study of ψ_4 and ψ_{21} is presented in Figure. (6.1) The study utilizes different constant sets of rate values of parameters; particularly, those of their means (

$\langle\psi_4\rangle$ and $\langle\psi_{31}\rangle$) standard deviations (σ_4 and σ_{31}), and autocorrelation times (τ_4 and τ_{31}). Subsequently, the results attained when using model (Güler, 2015) are taken relative to the relevant microscopic simulation results; they show that with remarkable accuracy, this model predicts $\langle\psi_4\rangle$, $\langle\psi_{31}\rangle$, σ_4, and σ_{31} almost same for models. Such precise accuracy is missing, however, in its prediction of autocorrelation times, which itself still enjoys a high degree of accuracy.

The use of these models can contribute to the implementation of a realistic the neuron in technology. We used C++ programming which is developed by Güler, with some minor modification and MATLAB has been used for plotting the results.

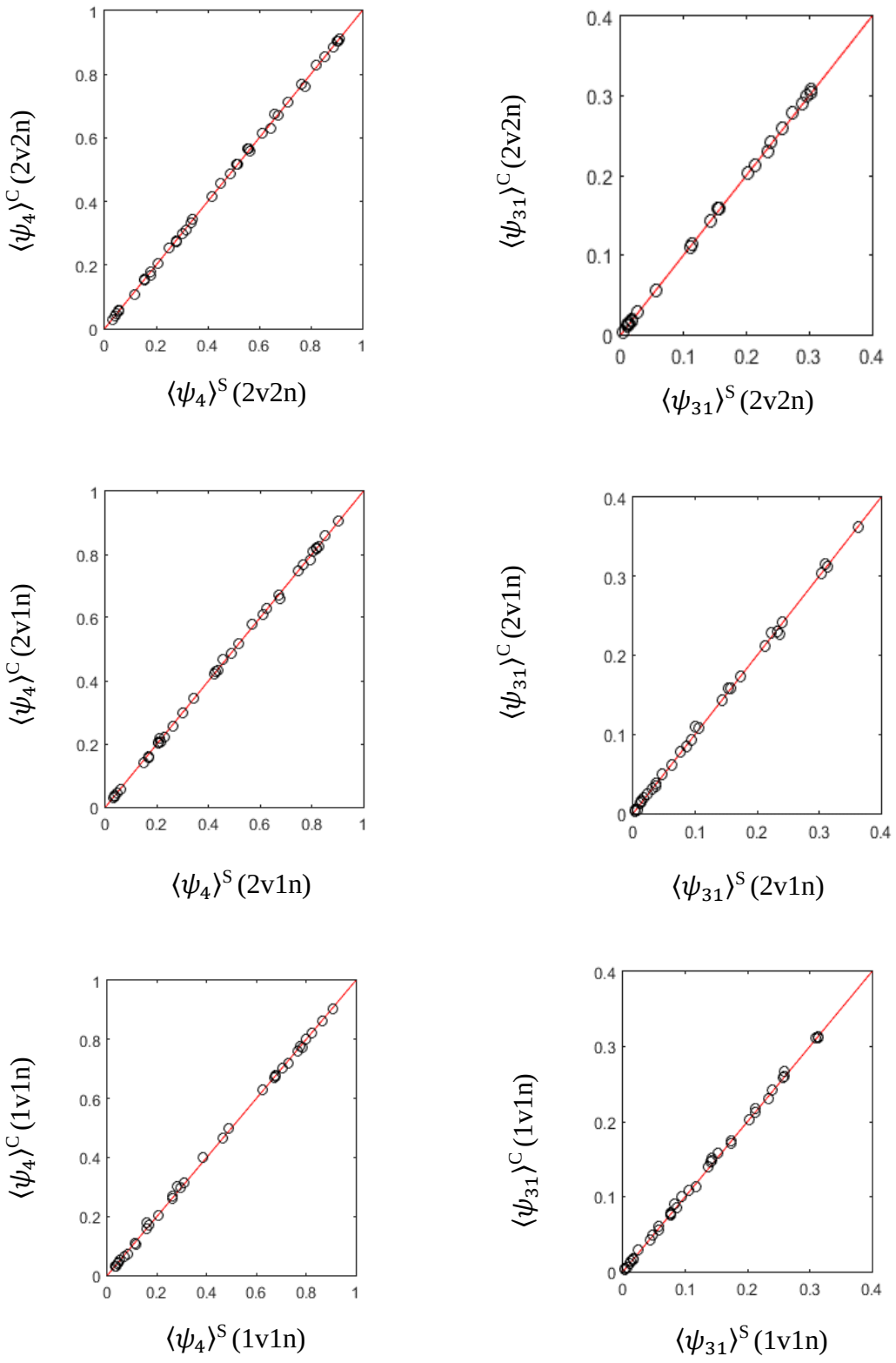

Figure 6.1: Various experiments that have proving the value of the model Güler (2015) using conductance's for 1000 sodium channels and 300 for potassium channels clusters for all three models 2v2vn, 2v1n and 1v1n.

Figure 6.1 shows the various experiments that have been conducted for 300 potassium channel and 1000 sodium channel clusters that have been conducted in the hopes of proving the value of the model of paper Güler (2015). For the potassium experiments, we used a series of sixty randomly generated rate values. A number of different statistical observables are calculated using for all three models 2v2vn, 2v1n and 1v1n. Using set of sixteen randomly generated rate value observed of {α_n is in the set (0:1); β_n is in the set (0:0.5)} used for potassium; for the sodium channels, were placed in the space of [α_m is in the (0:1); β_m is in the set (0:0.5); α_h is in the set (0:1); β_h is in the set (0:0.5)] was used. (denoted by superscript C) using these rate tuples; these observables are also compared to the relevant measurements for the microscopic simulation (denoted by the superscript S). Additionally, the autocorrelation time and standard deviation are respectively denoted by τ and σ. The perfect match between the microscopic simulation and the present model is illustrated by a linear line. The linear line was added to provide guidance in each of the plots; expectation values were calculated using a 400s time window.

Another numerical experiment we conducted (Güler, 2015) concerns the HH type membrane's spiking frequencies. The following differential equation is used to calculate the evolution of the transmembrane voltage (V) overtime in equation 6.4.

$$\dot{CV} = -g_K\psi_4\,(V - E_K) - g_{Na}\psi_{31}\,(V - E_{Na}) - g_L\,(V - E_L) + I \qquad (6.4)$$

Where the input current is represented by I. The constant membrane parameters' values are: the voltage-dependent membrane capacitance (contained in Table 4.1) and rate function of the membrane provided in Chapter (4).

(a)

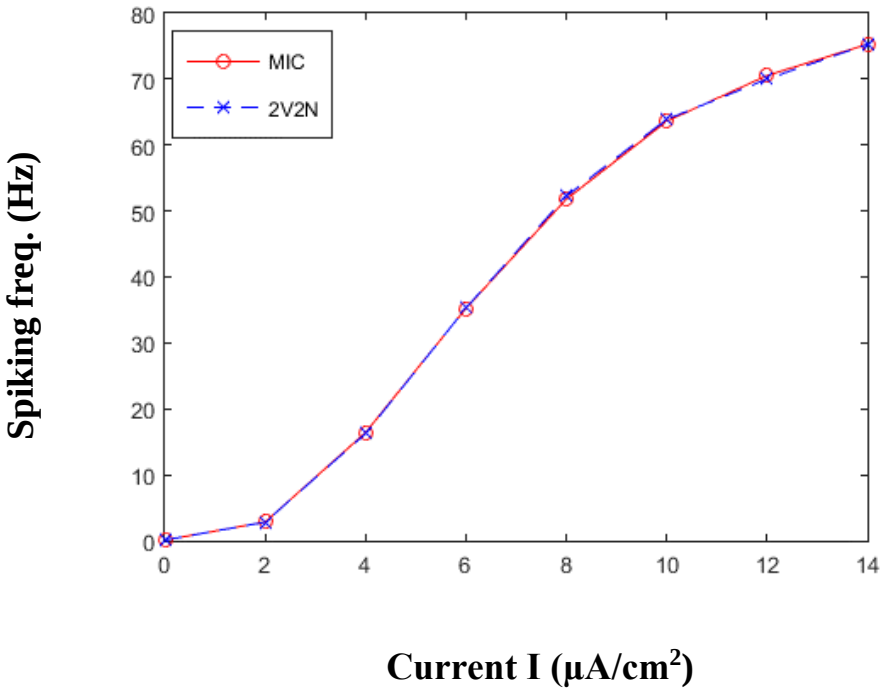
MIC
2V2N
Spiking freq. (Hz)
Current I (μA/cm²)

(b)

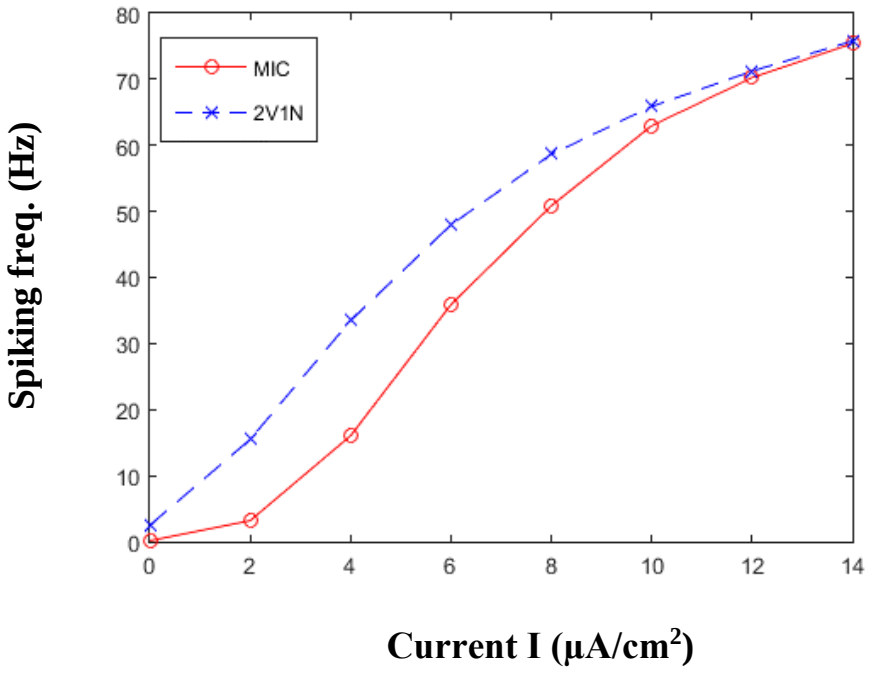
MIC
2V1N
Spiking freq. (Hz)
Current I (μA/cm²)

(c)

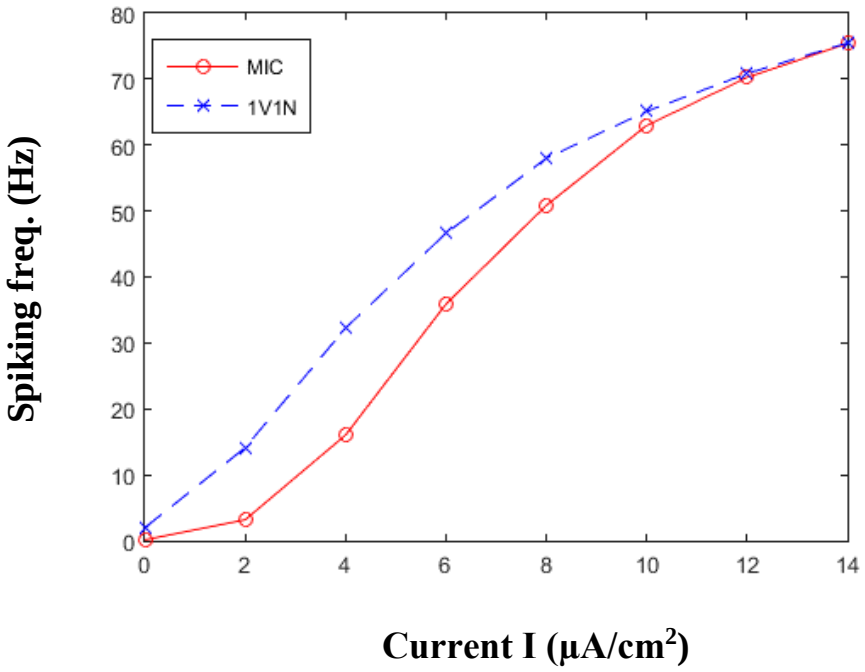
MIC
1V1N
Spiking freq. (Hz)
Current I (μA/cm²)

(d)

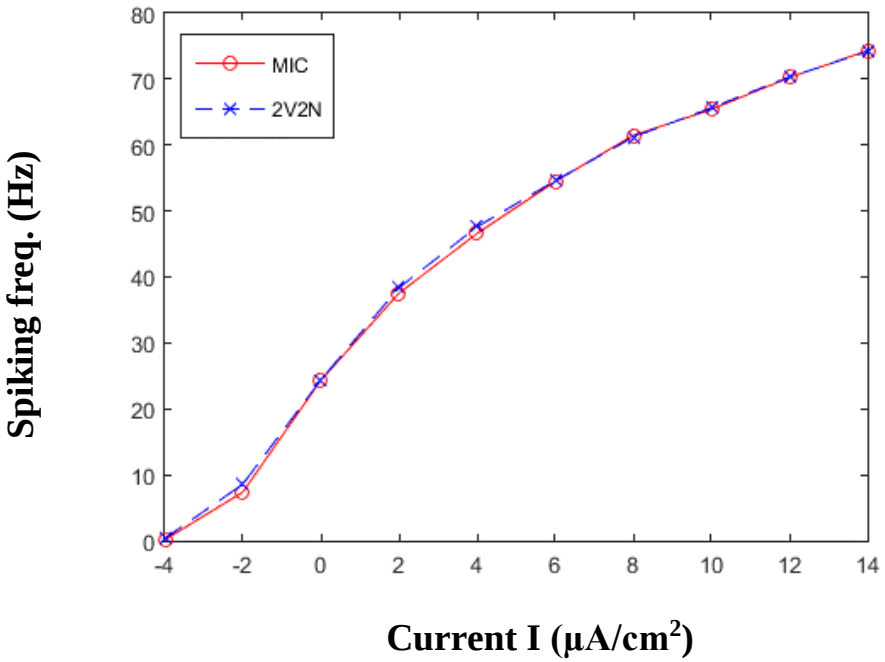
MIC
2V2N
Spiking freq. (Hz)
Current I (μA/cm²)

(e)

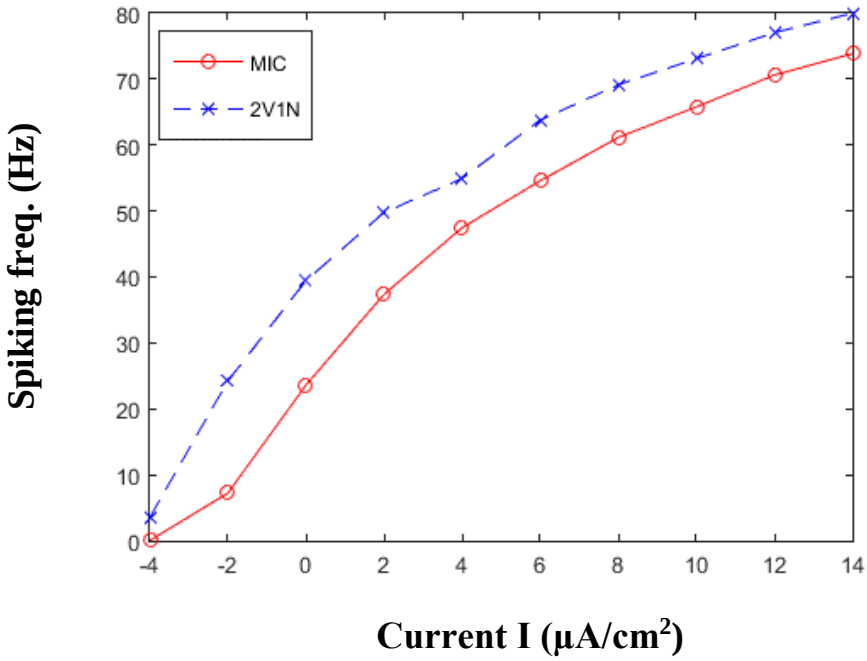

(f)

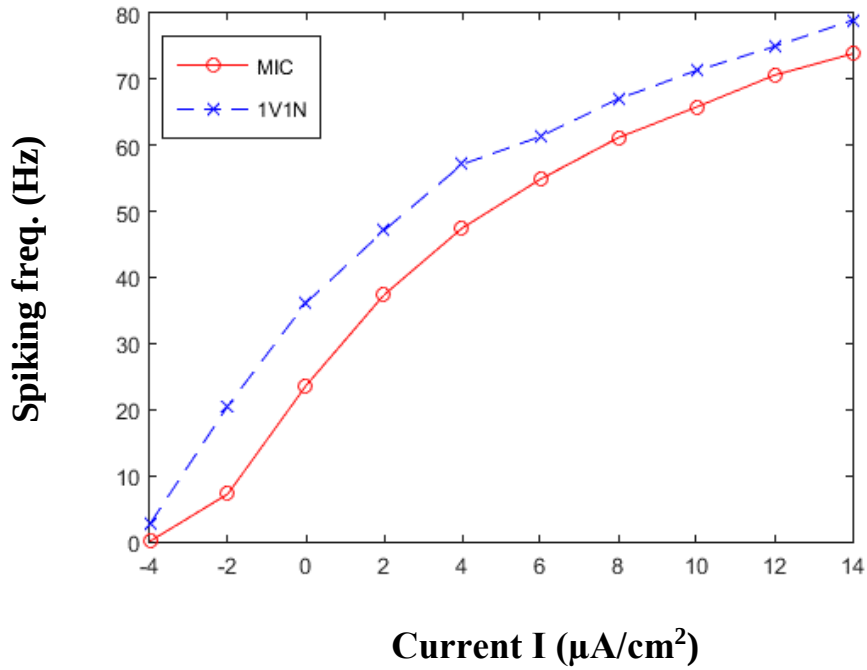

Figure 6.2: Mean spiking rates versus the input current, exposed by a membrane patch.

Fig. 6.2 shows the spiking frequencies versus input current corresponding to two sizes of membranes. The result of the Mean Spiking Freq. rates versus the amount of input

current, demonstrated by a membrane patch comprising (a), (b) and (C) were used 7, 200 potassium channels for all three graphs and the number of sodium channel is 24, 000 and (d), (e) and (f) 720 potassium channels and 2, 400 sodium channels comprising from the microscopic simulations and calculation from the 2v2n, 2v1n and 1v1n models respectively. One plot for every figure corresponds either to a result of the microscopic simulations or the calculation of the 2v2n, 2v1n and 1v1n models, respectively. The averages were calculated over a period of 50s. It is evident that the model of paper (Güler, 2015) resulting frequencies correspond greatly with those of the microscopic simulations. While the transition rates were previously taken as constant in the minimal diffusion (MD) model or 2v2n model, the present rates are altered sporadically during spiking due to their voltage-dependent nature. Regardless, what really matters for an action potential to start is the sub-threshold activity; said activity changes very little within that phase and so the model remains applicable for 2v2n model. Furthermore, the other two model are closed together 1v1n model is more closed to microscopic simulation than, the 2v1n model. Güler (2011) showed that changes in the number of open channels and transmembrane voltage fluctuations in the phase of sub-threshold activity share a non-transient correlation. Known as NCCP, this phenomenon has been found to be a major reason for limited-size neuronal membranes' increased excitability and spontaneous firing. Finite and pivotal to the existence of NCCP, the autocorrelation time for the number of open channel fluctuations must not equal zero. (Güler, 2015)'s model accuracy in representing the spiking frequencies shown in Figure 6.2 illustrates how efficient and exact it is in finding autocorrelation times and fluctuation amplitudes.

6.2 Experiment results

The present study assesses 2v2n, 2v1n, and 1v1n formulations by taking them in conjunction with the precise microscopic Markov simulation; specifically, this is done by considering the specific standard deviation and autocorrelation time of the relevant state density ψ_0. τ is taken to represent the autocorrelation time provided it complies with the following equality:

$$\frac{\langle \phi_0(t)\phi_0(t+\tau)\rangle}{\langle \phi_0^2(t)\rangle} = e^{-1} \tag{6.5}$$

Where the time t accommodates the attainment of an equilibrium. Hence, 60 sets of measurements have been taken by way of distinct randomly-generated transition rate matrices for each set. ψ_k for simulation it is exact simulation, the result is computed for both model 2v1n and 1v1n of each data. After modifying original model minimal diffusion by using ion channel dynamic according to input voltage for both model 2v1n and 1v1n. And taking the average density fluctuation for number of open and close ion channel for example for potassium or sodium. At the same time, it is the average ratio for potassium. We can get the result after it is computed from the exact microscopic simulation.

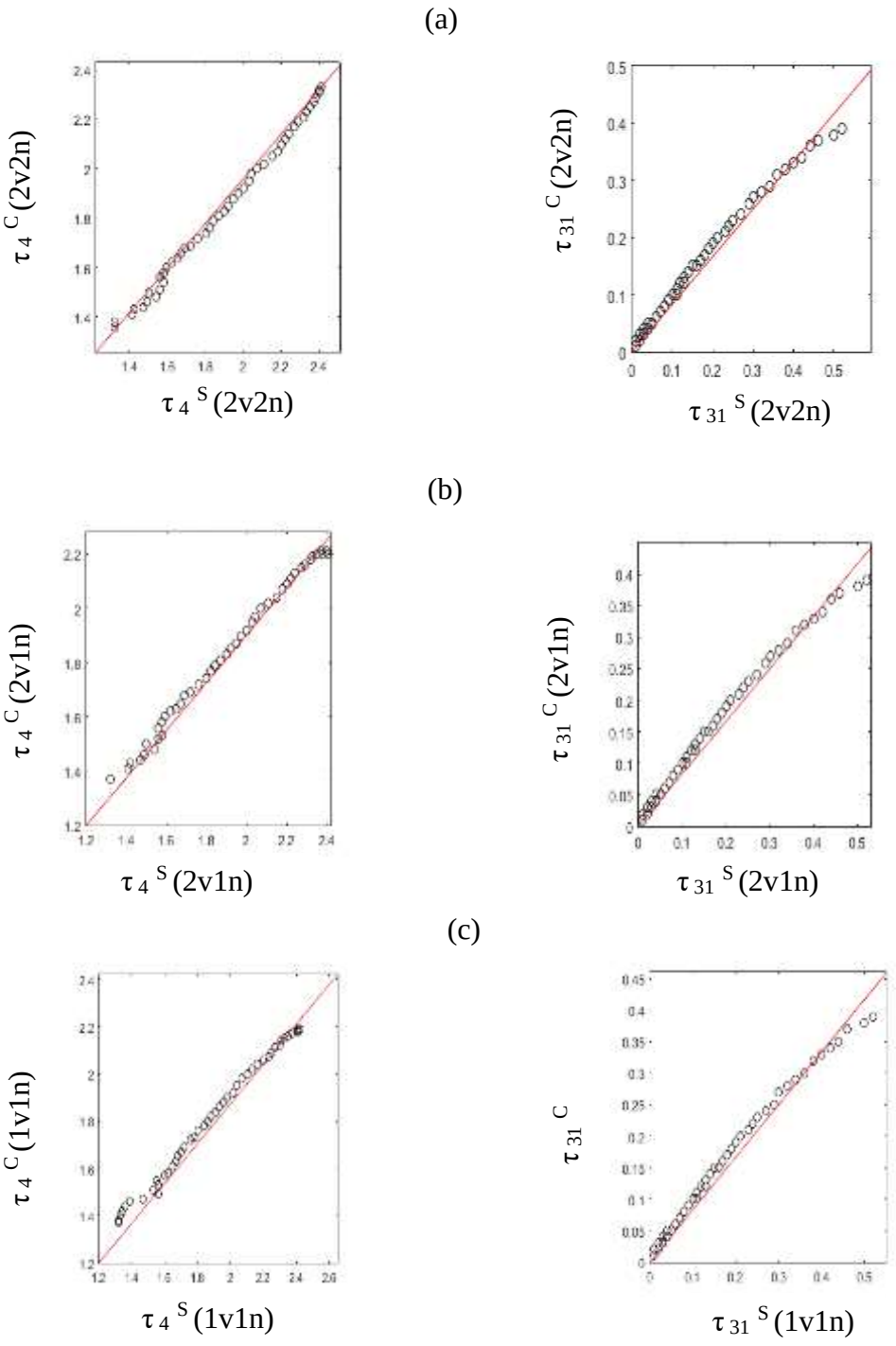

Figure 6.3: The relevant state autocorrelation times calculated for the (a) 2v2n, (b) 2v1n, and (c) 1v1n formulations (respectively corresponding to τ2v2n, τ2v1n, and τ1v1n).

Figure 6.3 Shows that the microscopic standard deviation is predicted with an impressive degree of accuracy in all three of the models (2v2n, 2v1n, and 1v1n); also illustrated the calculated for the formulations corresponding to τ2v2n, τ2v1n, and

τ1v1n in comparison to those acquired from the microscopic Markov simulation (represented by τ_s). By using a collection of independently-evolving Markov chains, when each developing autonomously under the state transition diagram provided in Figure (3.1) and figure (3.2) in chapter (3). A different transition matrix was used to measure a total 60 sets of autocorrelation time, where for each of the randomly-generated matrix elements of a value between 0 and 0.5 in each of the sets. Whereas the strategically-placed straight line is proposed to point to the exact similarity among the model and the microscopic simulation. The models are similar to the equivalent exact microscopic simulation. In regards to the autocorrelation times, also figure 6.3 shows that the results obtained from 2v2n and 2v1n are practically the same while that of the 1v1n formulation was notably different. These results were anticipated because, while the 2v1n formulation was formulated such that it gave results similar to those of the original 2v2n model, the 1v1n was only supposed to provide first–order accuracy relative to the 2v2n model's autocorrelation time. Furthermore, it is evident that where microscopic simulations are concerned, the autocorrelation times provided by both the 2v2n models are more accurate than those in the 1v1n and 2v1n model, in the same time 1v1n closer to the microscopic simulation than 2v1n. This is believed to be the case because, relative to their relevant microscopic autocorrelation time-measurements, the majority of the measurements in the 1v1n model are somewhat biased (at an average of 10%) towards smaller values. Based on the equations provided by Güler (2016) and Equation (6.5), it is evident that the number of Markov chains N has little to no impact on the autocorrelation time. In providing evidence in support of this, the autocorrelation times of a variety of N values were measured for both the microscopic simulations and (Güler, 2016) models; it was revealed that they were independent of the size of the ensemble.

Chapter 7

CONCLUSION

This thesis has shown that in a membrane with a limited area, the function of the cell is significantly affected by whether or not each of the ion channels has multiple gates. This multiplicity, in addition to inducing spike-coherence-enhancing NCCP, is one of the primary reasons for the increase in spontaneous firing and excitability of smaller neuronal membranes (as it often results in non-trivially persistent membranous cross correlations). Güler (2011) discovered that even in relatively larger membranes where the gate noise is insufficient to activate the cell, spontaneous firing continues to be facilitated by NCCP, which also improves spike train consistency. As such, NCCP is expected to play a primarily facilitative role where synaptically-joined neurons – specifically their synchronization over time – are concerned. Further investigation is warranted into the role of NCCP for noisy input and time varying currents, as they relate to stochastic resonance. The argument that the mere introduction, into deterministic HH equations, of certain white noise terms with vanishing means was insufficient to allow the modelling of size-limited cell dynamics beyond a particular level of accuracy was made by this thesis. Furthermore, channel variables in said equations need to be renormalized into a new strand of functional forms that depend on the particular voltage in question.

Stochastic HH equations are incapable of satisfactorily capturing NNCP despite their relatively accurate spike generation statistics. Güler (2011) suggests that this may be

remedied by supplanting the conductances with a few additive colored noise terms. In this thesis, white noise terms for the gating variables in Langevin equations were used in the implementation of the gate noise. A series of numerical experiments were subsequently conducted by utilizing expressed equations under constant stimulus and stimuli pulses. The resulting values for spike coherence and generation, jitter, and firing efficiency were found to correspond to those gotten from the exact microscopic Markov simulations. These observations lend credence to the importance of NCCP and explicitly demonstrate that the inadequacy inherent to FL equations has little bearing on the present formulation, the equations of which are essentially a generalized form of the HH equations for limited-size membranes.

Güler (2011) argued that rather than implementing NCCP using colored noise terms in the conductance's, channel variables could alternatively be renormalized into certain functional forms that are determined by the voltage in question. This method incorporates certain analytical terms such that the parameters $\Omega_K^V - \Omega_{Na}^V$ VK and V Na are used to acquire proper non-vanishing values, as opposed to simply adding colored noise terms. The question of which functional forms are capable of accurately reflecting NCCP remains open, despite the availability of a renormalization scheme in Güler (2011). The model outlined in this thesis could offer some useful insight into the role of NCCP as it relates to spike propagation and the very nature of said propagation. The individual channels were taken to be linked to their surrounding channels, such that the opening of surrounding channels increased the probability of and individual opening. This cooperation shares some similarities with the non-zero autocorrelation time characteristic of NCCP generation in sodium channels – represented by the construct $\psi_{Na}^L - m^3h$. It would be unwise, however, to postulate the existence of a

shared biophysical ground as neither the NCCP framework, nor the autocorrelation construct, display any cooperation between each neighboring channels (or the reliance of a channel's opening on how open surrounding channels are). Regardless, both phenomena may have related effects on how action potentials are initiated since NCCP is known to promote excitability.

A theoretical argument has been propounded here for the purpose of deriving the formulation and positing criteria (to be encapsulated in any approximation scheme) useful in determining both the parameter values and the attendant noise variances. The formulation manifests itself as a pair of diffusively-coupled Langevin-type equations and is advantageous due to its inherent simplicity. The density of transition matrix and the state space are irrespective of the size, as well as it accounts for just two stochastic variables and their corresponding noise terms while also overcoming potential restrictions imposed by the matrix square root. Consequently, the effects of fluctuations in the densities of all states other than the relevant state were taken as a collective as opposed to individually. The efficiency of (Güler, 2016) model as it relates to clusters of sodium and potassium channels and limited-size membrane excitability has been proven. Efforts are presently underway to analytically evaluate the relevant state density's probability function and extend the formulation to include cases with a random number of relevant states.

This thesis aimed to explicate the properties of the minimal diffusion formulation, which is here termed the 2v2n model. It began, first, with analyzing the autocorrelation function for the density of the relevant state using the aforementioned formulation; the autocorrelation was found to be represented by a pair of exponentially decaying additive terms. What followed was the introduction of two diffusion models – 1v1n

and 2v1n, containing just one noise term each. While they approximated the 2v2n model's dynamics for sodium and potassium, both models also adversely affected its structural complexity. The 1v1n model, despite being first-order time gap accurate, has one less stochastic variable and is thus less accurate than the 2v1n model, whose autocorrelation function is equal to the 2v2n model's autocorrelation function. The theoretical analysis is supported by numerical simulations, which were also provided. The 1v1n and 2v1n models facilitate the computation of the Markov chain ensembles' collective fluctuations, even further than the minimal diffusion formulation. Their lack of complexity also makes them potentially useful for the analysis and promotion of Markov chain ensembles' collective evolution. The 1v1n and 2v1n formulations are better suited for qualitative and quantitative analysis respectively. As with all other diffusion formulations, the minimal diffusion formulation (of which the 1v1n and 2v1n models are variants) is not suitable for dynamics absent at equilibrium. It is for this reason that the analysis assumed the transition rates to be constant since equilibrium would have been difficult to reach if the rates were allowed to change rapidly.

Both $\langle \psi_s \rangle$ and $\langle \psi_r \rangle$ were used in the formulation without commanding the steady-state condition $\alpha\langle \psi_s \rangle = \beta\langle \psi_r \rangle$. This was necessary to ensure that the models remained valid even in conditions with slow-varying transition rates. When steady-state conditions are used in formulating a Markov diffusion model (like that in Ref. Linaro and Storace…, 2011), the resulting model is rendered inaccurate under noisy transition rates Güler, (2013b) or at non-equilibrium (Orio and Soudry, 2012). Although, consider the case of study the variant formulation 2v1n and 2v1n gives equivalent results, but 1v1n although good enough is less accurate corresponding to the 2v2n and

2v1n. Even though, the two model 2v1n and 1v1n were closed together but 2v2n which is term of minimal diffusion still better than them.

REFERENCES

Adair, R. K. (2003). Noise and stochastic resonance in voltage-gated ion channels. *Proceedings of the National Academy of Sciences*, 100(21), 12099-12104.

Almassian, A., & Güler, M. (2011, June). Detection of time varying signals by the dissipative stochastic mechanics based neuron model. In *AIP Conference Proceedings* (Vol. 1371, No. 1, pp. 83-91). AIP.

Baxendale, P. H., & Greenwood P. E. (2011). Sustained oscillations for density dependent Markov processes. *Journal of mathematical biology*, 63(3), 433-457.

Callahan, M. J., & Korn, S. J. (1994). Permeation of Na+ through a delayed rectifier K+ channel in chick dorsal root ganglion neurons. *The Journal of general physiology*, 104(4), 747-771.

Chow, C. C., & White, J. A. (1996). Spontaneous action potentials due to channel fluctuations. *Biophysical journal*, 71(6), 3013-3021.

Chung, S. H., Anderson, O. S., & Krishnamurthy, V. V. (Eds.). (2007). *Biological membrane ion channels: dynamics, structure, and applications*. Springer Science & Business Media.

DeFelice, L. J., and Isaac, A. (1993). Chaotic states in a random world: Relationship between the nonlinear differential equations of excitability and the stochastic properties of ion channels. *Journal of Statistical Physics*, 70(1), 339-354.

Fox, R. F., & Lu, Y. N. (1994). Emergent collective behavior in large numbers of globally coupled independently stochastic ion channels. *Physical Review* E, 49(4), 3421.

Gerstner, W. Kistler; WM (2002). Spiking Neuron Models. Single Neurons, Populations, Plasticity.

Güler, M. (2007). Dissipative stochastic mechanism for capturing neuronal dynamic under the influence of ion channel noise: Formalism using a special membrane. *Physical Review* E, 76(4), 041918.

Güler, M. (2008). Detailed numerical investigation of the dissipative stochastic mechanics based neuron model. *Journal of Computational Neuroscience*, 25(2), 211-227.

Güler, M. (2011). Persistent membranous cross correlation due to the multiplicity of gates in ion channels. *Journal of computational neuroscience*, 31(3), 713-724.

Güler, M. (2013a). Stochastic Hodgkin equations with colored noise terms in the conductances. *Neural computation*, 25(1), 46-74.

Güler, M. (2013b). An investigation of the stochastic Hodgkin-Huxley models under noise rate functions. *Neural computation*, 25(9), 2355-2372.

Güler, M. (2015). Minimal diffusion formulation of Markov chain ensembles and its application to ion channel clusters. *Physical Review* E, 91(6), 062116.

Güler, M. (2016). Efficient variant of the minimal diffusion formulation of Markov chain ensembles. *Physical Review* E, 93(2), 022123.

Goldwyn, J. H., Imennov, N. S., Famulare, M., & Shea-Brown, E. (2011). Stochastic differential equation models for ion channel noise in Hodgkin-Huxley neurons. *Physical Review E*, 83(4), 041908.

Hertz, J. A., Krogh, A. S., & Palmer, R. G. (1991). *Introduction to the theory of neural computation* (Vol. 1). Basic Books.

Hille, B. (2001). *Ion channels of excitable membranes* (Vol. 507). Sunderland, MA: Sinauer.

Hodgkin, A. L., & Huxley, A. F. (1952) A quantitative description of membrane current and its application to conduction and excitation in nerve. *The Journal of Physiology*, 117(4), 500-544.

Hoppensteadt, F. C., & Izhikevich, E. M. (1997). Weakly Connected Neural Networks.

Inzikevich, E. M. (2007). *Dynamical system in neuroscience*. MIT press

Izhikevich, E. M. (2000). Neural excitability, spiking and Bursting. *International Journal of Bifurcation and Chaos*, 10(06). 1171-1266.

Jung, P., & Shuai, J. W. (2001). *Optimal sizes of ion channel clusters. EPL (Europhysics Letters)*, 56(1), 29.

Koch, C. (2004). *Biophysics of computation: information processing in single neurons*. Oxford university press.

Kolb, B., & Whishaw, I. Q. (2009). *Fundamentals of human neuropsychology*. Macmillan.

Kurtz, T. G. (1978). Strong approximation theorems for density dependent Markov chains. *Stochastic Processes and their Applications*, 6(3), 223-240.

Lecar, H., & Nossal, R. (1971). Theory of threshold fluctuations in nerves: II. Analysis of various sources of membrane noise. *Biophysical journal*, *11*(12), 1068-1084.

Linaro, D., Storace, M., & Giugliano, M. (2011). Accurate and fast simulation of channel noise in conductance-based model neurons by diffusion approximation. *PLoS Comput Biol*, 7(3), e1001102.

Lytton, W. W. (2002). Computational Neuroscience and You. From Computer to Brain: *Foundations of Computational Neuroscience*, 11-23.

Mélykúti, B., Burrage, L., & Zygalakis, K. C. (2010). Fast stochastic simulation of biochemical reaction system by alternative formulation of the chemical Langevin equation. *The Journal of chemical physics,* 132(16), 164109.

Orio, P., & Soudry, D. (2012). Simple, fast and accurate implementation of the diffusion approximation algorithm for stochastic ion channels with multiple state. *PloS* one, 7(5), e36670.

Rowat, P. F., & Elson, R. C. (2004). State-dependent effects of Na channel noise on neuronal burst generation. *Journal of Computational Neuroscience*, 16(2), 87-112.

Rowat, P. F., & Greenwood, P. E. (2014). The ISI distribution of the stochastic Hodgkin-Huxley neuron. *Frontiers in Computational Neuroscience*, 8.

Saarinen, A., Linne, M. L., & Yli-Harja, O. (2008). Stochastic differential equation model for cerebellar granule cell excitability. *PLoS Comput Biol*, 4(2), e1000004.

Sakmann, B., & Neher, E. (1995). Single-channel recording, 2nd edn Plenum. *New York*

Schmandt, N. T., & Galán, R. F. (2012). Stochastic-shielding approximation of Markov chain and its application to efficiency simulate random ion-channel gating. *Physical Review letter* 109(11), 118101.

Sherwood, L. (2011). *Fundamentals of human physiology*. Cengage Learning.

Softky, W. R., & Koch, C. (1993). The highly irregular firing of cortical cells is inconsistent with temporal integration of random EPSPs. *Journal of Neuroscience*, 13(1), 334-350.

Strassberg, A. F., & DeFlice, L. J. (1993). Limitations of Hodgkin-Huxley formalism: effect of single channel kinetics on transmembrane voltage dynamics. *Neural computation*, 5(6), 843-855.

Tuckwell, H. C. (1989). *Stochastic processes in the neurosciences*. Society for industrial and applied mathematics.

White, J. A., Klink, R., Alonso, A., A. R. (1998). Noise from voltage-gated ion channels may influence neuronal dynamic in entorhinal cortex. *Journal of neurophysiology*, 80(1), 262-269.

Zeng, S., & Jung, P. (2004). Mechanism of neuronal spike generation by small and large ion channel cluster. *Physical Review* E 70(1), 011903.

Zwanzig, R. (2001). *Nonequilibrium statistical mechanics*. Oxford University Press.